Understanding the mechanism of IGF-1R ligand binding and activation

By

Arun Babukuttan

(Master of Biotechnology)



Supervised by Professor Briony Forbes

Proteins in Metabolism and Cancer Laboratory

Discipline of Medical Biochemistry

College of Medicine and Public Health, Flinders University

Title of thesis
Understanding the mechanism of IGF-1R ligand binding and activation
Full name of student
Arun Babukuttan
Any degree student currently hold
Bachelor of Science, Biotechnology
Name of the college
College of Medicine and Public Health, Flinders University
Name of degree this thesis is being submitted for
Master of Biotechnology

Date of submission

2nd June, 2025

Table of Contents

ABSTRACT	iii
DECLARATION OF ORIGINALITY	iv
ACKNOWLEDGEMENTS	v
LIST OF ABBREVIATIONS	vi
LIST OF FIGURES	ix
LIST OF TABLES	X
CHAPTER 1: INTRODUCTION	1
1.1 IGFs and its biological functions	1
1.2 IGF-1R and its biological functions	3
1.3 Overexpression of IGF-1R causes cancers	4
1.4 Overexpression of IGF-1R in Colorectal Cancer (CRC)	4
1.5 Overexpression of IGF-1R in Brest Cancer (BC)	5
1.6 Structure, regions and binding sites of IGF-1R	6
1.7 Overview of IR activation	7
1.8 Hypothesized IGF-1R activation	7
1.9 Study hypotheses and aims	10
1.9.1 Study Hypotheses	11
1.9.2 Aims	11
CHAPTER 2: MATERIALS AND METHODS	12
2.1 Materials	12
2.1.1 DNA Cloning and molecular biology	12
2.1.2 Protein expression and quantification	16
2.2 Methods:	20
2.2.1 Bacterial cloning	20
2.2.2 Cell culture and transfection of IGF-1R gene mutants	24
2.2.3 Separation of proteins using SDS PAGE and quantitation of IGF-1R mutant's expre	ssion 26
CHAPTER 3: RESULTS	29
3.1 Cloning of IGF-1R FnIII-I domain mutants and K530A into pcDNA3.1+ IGF-1R mammexpression vector	
3.1.1 Cloning Strategy:	
3.1.2 Ligation of designed IGF-1R mutant gene fragments into PGEM-T easy cloning vec	ctor: . 30
3.1.3 Restriction of digestion of pGEM-T easy + IGF-1R mutant g-block and their gel ext	
3.1.4 Successful ligation of pcDNA3.1 expression vector with IGF-1R mutant inserts:	
3.1.5 Sanger sequencing of pcDNA3.1+ IGF-1R FnIII-I domains:	35
3.2 Cellular expression and activation IGF-1R FnIII-I mutant domains	36
3.2.1 Transfection of pcDNA3.1+ IGF-1R FnIII-I domain mutants into DKO cells:	36

	3.2.2 Expression of IGF-1R FnIII-I domain mutant receptors in DKO cells:	36
	3.2.3 Activation of IGF-1R FnIII-I domain mutant receptors in DKO cells:	36
C	HAPTER 4: DISCUSSION	39
	4.1 Successful cloning of IGF-1R FnIII-I domain mutants into mammalian expression vector pcDNA3.1	39
	4.2 Expression and activation of IGF-1R FnIII-I domain mutants in DKO cells:	39
	4.3 Future Direction:	40
	4.4 Conclusion.	41
	Reference	42

ABSTRACT

This project set out to better understand how a protein called the insulin-like growth factor 1 receptor, or IGF-1R, actually works inside our cells. IGF-1R is really important—it helps control how our cells grow, divide, and survive. It's especially active during childhood growth but also plays a role in tissue repair and even some cancers. Scientists already know quite a bit about how IGF-1R is activated, but there are still some pieces of the puzzle missing, especially about certain areas of the protein that may help it bind to its partners (IGF-I and IGF-II).

In this study, we focused on a specific part of the receptor known as the FnIII-I domain, which might act as a kind of secondary binding site. To test this idea, we made precise changes (mutations) to four amino acids that we thought might be important. We then inserted these modified genes into human cells that don't normally produce IGF-1R and checked whether the receptor still worked when stimulated.

What we found was pretty exciting—mutations at three of these sites made the receptor less responsive to stimulation, and one of them nearly shut down activation completely. This tells us that these parts of the receptor are more important than we thought and likely help stabilize how the receptor binds to its ligands and switches "on."

In simple terms, this research helps fill in the blanks about how IGF-1R functions, which is really valuable not just for understanding biology but also for designing better drugs in the future—especially for diseases where IGF-1R is overactive, like cancer.

DECLARATION OF ORIGINALITY

I certify that this thesis: 1. does not incorporate without acknowledgment any material previously submitted for a degree or diploma in any university 2. and the research within will not be submitted for any other future degree or diploma without the permission of Flinders University; and 3. to the best of my knowledge and belief, does not contain any material previously published or written by another person except where due reference is made in the text.

Arun Babukuttan

02/06/2025

ACKNOWLEDGEMENTS

I would like to begin my acknowledgements by thanking my supervisor, Professor Briony Forbes. I'm extremely grateful to you for allowing me to complete my Research Project by giving me an opportunity to work in your laboratory. In these 9 months, I've gained lots of skills and knowledge from you. I'm eternally grateful to you for being patient and compassionate towards me even during my hard times.

I would also like to thank Allanah Merriman, who was there for me whenever I had any doubts regarding experimental protocols and trained and assisted me during my initial laboratory days. Your constant reminder of noting down each and everything came handy for me while writing down my methods and interpreting my results.

Along with that, I would also like to thank my recent laboratory mate, Janvi Shah. Even though you started your scholarship in later part of my research, your presence in the laboratory was always appreciated. You have helped me during my research not only by always maintaining a positive environment by your constant banter but also helping me by assisting me in my research.

My biotechnology cohort was also incredible. I would like to thank them all for sharing each other's progress and struggles we were going through together. In my cohort, I'm extremely thankful to Raisa Mahboob, Rohan Khatri, Rushita Savaliya and Janvi Patel for keeping a check on me when I was going through a hard time during my research. You all have always been there for me to have a chat and check on my well-being.

Not only them but I'm also thankful to Mariya Francis from Biotech Feb 2023 cohort. Your words of affirmation and reassurance during the final stages of my research gave me a boost to mental strength.

In the end, I would like to thank my family and friends. I'm extremely thankful to my Mom and Dad as they've been giving me constant encouragement during my research and kept faith in me that I would successfully complete this program.

Also, I would like to thank my brothers who were available for me always whenever I was feeling stressed, wanted to rant or to distract my mind. A small chat with them never failed to refresh my mind.

LIST OF ABBREVIATIONS

IGF I and II	Insulin-like Growth Factor I and II
IGF-1R	Insulin-like Growth Factor Receptor 1
hIGF-1R	Human Insulin-like Growth Factor Receptor 1
WT IGF-1R	Wild Type Insulin-like Growth Factor Receptor 1
IR	Insulin Receptor
IR A and B	Insulin Receptor isoform A and B
RTK	Receptor Tyrosine Kinase
IGFBP	Insulin-like Growth Fcator Binding Protein
PI3K	Phosphoionositide 3-kinase
MAPK	Mitogen Activated Protein Kinase
ERK	Extracellular signal-Regulated Kinase
K/ Lys	Lysine amino acid
Arg	Arginine amino acid
Leu	Leucine amino acid
Pro	Proline
His	Histidine
Thr	Threonine
Ile	Isoleucine

Ser	Serine
3D	3-dimensional
°C	Degree celcius
bp	Base Pair
kb	Kilo Base
mM	Millimolar
μg	Micro ram
V/V	Volume/ volume
w/v	Weight/ volume
μL	Microlitre
rpm	Revolutions per minute
mins	Minutes
mL	Millilitre
ng	Nanogram
nm	Nanometre
μm	Micrometre
V	Volts
UV	Ultra Violet
pcDNA3.1+IGF- 1R (-X/K)	pcDNA3.1+IGF-1R double digested by XhoI and KpnI-HF

HEK 293FT DKO cells	Human Embryonic Kidney 293FT Double Knock Out cells	
DKO, Double K/O	Double Knock Out cells	
BSA	Bovine Serum Albumin	
TBST	Tris-Base Saline buffer with Tween 20	
Taq	Thermus aquaticus	
HEPES	4-(2-hydroxyethyl)-1-piperazineethanesulfonic acid	
PCR	Polymerase Chain Reaction	
Exp.	Experiment	
SDS-PAGE	Sodium Dodecyl Sulphate-Polyacrylamide Gel Electrophoresis	
kDa	Kilo Dalton	

LIST OF FIGURES

Figure 1.1	Schematic representation of insulin and IGF signalling pathways mediated through IR-A, IR-B and IGF-1R.	
Figure 1.2	Schematic representation of the stepwise ligand-induced activation of the IGF-1 receptor (IGF-1R).	
Figure 1.3	Structural visualization of key residues within the IGF-1R receptor involved in receptor-ligand interactions and putative site-2 interface	
Figure 3.1	Schematic representation of the cloning strategy applied to generate IGF-1R mutant gene fragments	
Figure 3.2	Agarose gel electrophoresis of restriction-digested pGEM-T easy vector containing IGF-1R mutant DNA fragments.	
Figure 3.3	Agarose gel electrophoresis showing double restriction digestion of pcDNA3.1+ wt IGF-1R with XhoI and KpnI-HF.	
Figure 3.4	Agarose gel electrophoresis showing restriction digestion of pcDNA3.1 vector with IGF-1R mutant constructs.	
Figure 3.5	Sanger sequencing chromatogram confirming the presence of Ser471Ala (S471A) mutation in the IGF-1R FnIII-I domain construct using ApE software	
Figure 3.6	Evaluation of IGF-1R expression and activation in wild-type (WT) and mutant receptors.	

LIST OF TABLES

Table 1.1	Table 1.1: Table of corresponding amino acid residues between the insulin receptor (IR) and IGF-1 receptor (IGF-1R) involved in receptor activation and ligand binding.			
Table 2.1	cDNA sequences of designed IGF-1R analogues. The restriction enzymes used in the g-block design have been highlighted (Nsil/Xhol/KpnI), while the specific codon mutation for each analogue has been highlighted in yellow.			
Table 2.2	Summary of primers used for molecular biology components of this study.			
Table 2.3	Summary of vectors utilised for this study.			
Table 2.4	Summary of bacterial strains utilised for this study.			
Table 2.5	Summary table for the list of buffers and solutions with their composition.			
Table 2.6	Summary of IGF-1R, IR, and cell signalling molecule antibodies used in this study.			
Table 2.7	Summary table for the list of buffers and solution with their composition,			

CHAPTER 1: INTRODUCTION

1.1 IGFs and its biological functions

Insulin and insulin-like growth factors or hormones such as IGF-I and IGF-II share some of the common characteristics like genetic sequences, 3D structures and an evolutionary background. My research primarily focuses on IGF system.

While the overriding organ for IGF-I synthesis is the liver, a few other organs can make these peptides in a peripheral manner. The production of IGF-I in the liver is largely controlled by growth hormone, IGF-II on the other hand is more growth hormone independent. In the course of pregnancy, IGF-II is mostly usually released by the placenta.

They do have three transmembrane glycoprotein receptors that have very close levels of homology (50–85% sequence homology) and through which they act. These glycoprotein receptors have been referred to as the IR and the IGF-1R (insulin and insulin-like growth factor-1 receptors) yet they have many other relatives in the receptor family also known as receptor tyrosine kinases or RTKs (Khandwala et al., 2000; Macháčková et al., 2019; Pavelić et al., 2003; Sélénou et al., 2022).

Insulin Growth Hormone (IGF-I) is a key peptide hormone that plays an important role in regulating growth, development, metabolism and tissue development. It is primarily synthesized in liver under the influence if growth hormone (GH) and regulated in circulation by IGF-binding proteins (IGFBPs). IGF-I exerts its biological effect by binding with insulin-like growth factor receptor 1 (IGF-1R). The activation of this receptor caused by IGF-I leads to several downstream signalling pathway such as phosphoionositide 3-kinase/ protein kinase B (PI3K/Akt) pathway and the mitogen activated protein kinase/ extracellular signal-regulated kinase (MAPK/ERK) pathway. These cascading pathways are responsible for cell proliferation, differentiation and migration. During childhood, IGF-I facilitates bone growth and in adults, supports maintenance of muscle mass and metabolic balance along with enhancing glucose uptake and inhibiting apoptosis. The biological activity of IGF-I is controlled by six high-affinity IGF-binding proteins (IGFBP1-6) by acting as carriers controlling the spatial and temporal activity of IGF-I. Over-activation of IGF-IR caused by IGF-I causes several oncogenic transformation and tumor progression in several cancers while, inadequate IGF-I levels in body leads to retardation of growth and metabolic dysfunctions such

as insulin resistance and cardiovascular diseases (Blyth et al., 2020, Macháčková et al., 2019 Uchikawa et al., 2019).

Figure removed due to copyright restriction.

Figure 1.1: Schematic representation of insulin and IGF signalling pathways mediated through IR-A, IR-B and IGF-1R. The diagram illustrates different downstream signalling pathways initiated by insulin, IGF-I and IGF-II by binding to their respective receptors leading to receptor trans-autophosphorylation followed by activation of PI3K/Akt or Ras/MAPK pathway. Image sourced from (Blyth et al., 2020).

IGF-II acts through three different receptor complexes - insulin receptor (IR) type I isoform (IR-A) and insulin-like growth factor 1 receptor (IGF-1R) separately and a hybrid receptor of IGF-1R and IR-A. The high affinity of IGF-I and IGF-II binding to the IGF1R suggests that this receptor accomplishes most of the IGF-II-induced effects. When IGF-I or IGF-II binds to the IGF-1 receptor (IGF-1R), it will stimulate the downstream MAP kinase and PI3 kinase signalling pathways. (Khandwala et al., 2000; Macháčková et al., 2019; Pavelić et al., 2003; Sélénou et al., 2022)

Many of its biological functions are both tissue-specific and developmentally regulated. IGF-II is prominently expressed in the foetal organs, where the gene expression is also promoted by tissue-selective groups of promoters, thus it is significantly involved in the development and differentiation of the tissues that are the derivatives of the mesoderm. In the case of insulin, where the binding leads to glucose utilization, IGF-II specifically binds to IR-A leading to

mitogenesis. Following ligand binding, IGF-II behaves just like insulin and IGF-1 in the IGF1R. It activates the insulin receptor tyrosine kinases (RTKs) activity that is associated with its beta sub unit through which the intracellular signal is initiated. IGF-II stimulation of cell multiplication and prolonging cell life can be observed not only in individual cells, but a higher organizational level as well, for example, in promoting the bone growth by controlled differentiation and maturation of chondrocytes and some other cells of the perichondrium. Additionally, it also intervenes in the maintenance, maturation, and adaptation of cross-striated skeletal muscle tissues (Blyth et al., 2020; Livingstone, 2013; Sélénou et al., 2022).

1.2 IGF-1R and its biological functions

The receptor for IGF-I, known as IGF-1R, is a membranous form of protein structure with subunits that are hetero-tetramer formed by two α and two β units. This receptor is very similar to the insulin receptor in terms of protein sequence with which it shares around 60% homology. Just like the insulin receptor, it has a tyrosine kinase activity. Moreover, the IGF-1R is a subset of a receptor superfamily of tyrosine kinases that consists of the insulin receptor and another receptor orphan insulin receptor-related receptor (IRR). It displays high affinity to binding IGF-I and initiates both biochemical and physiological responses to this ligand in living organisms. The receptors also have some IGF-II binding ability, but to a much lesser extent, in explaining how it contributes to some of the effects of IGF-II during the growth phase of the foetus. It is now fairly common knowledge that IGF-1R signal transduction was first and foremost studied in the context of its contribution to growth hormone mediate postnatal growth. Specifically, IGF-1R and other insulin receptor subtypes present in that growth hormone belongs to the family of receptors that contain disulphide linked covalent structures. The fact that interacts with receptors rather as ligands in an incompletely understood conformational change is critical because almost all other receptors mediate signalling by receptor oligomerisation (Adams et al., 2000). The insulin receptors exist in two isoforms i.e., IR-A that is exclusive of exon 11 and has about 15% the activity of IGF-II binding that it does for insulin, higher than that which IR-A binds IGF-I with (Belfiore et al., 2017).

The IGF-1R typically has a pivotal role in the normal physiological setting since it controls cellular proliferation and differentiation and prevents apoptosis. When the IGF-1R is disrupted in mice, they exhibit retardation in foetal growth with consequent disorganization of skeletal muscle, skin, bone, and the nervous tissues. Enhanced IGF-1R expression has been documented in multiple tumour types in humans and blockade of this receptor enhances the transformed properties in certain tumour cell lines using techniques like antisense

oligonucleotides, monoclonal antibodies, or dominant negative mutations. Thus, the use of the IGF-1R as a target for cancer treatment has attracted some attention (Favelyukis et al., 2001).

1.3 Overexpression of IGF-1R causes cancers

Overexpression of IGF-1R has been observed to cause many types of cancers including Colorectal Cancer (CRC) and Breast Cancer (BC). Thus, many therapeutic researches are going on to mitigate this overexpression by targeting IGF-1R.

It has been shown that signals via IGF-1R are important in cell adhesion, migration, invasion, angiogenesis, and metastasis growth within distant organs. Depending upon the cell type studied, IGF-1R effects are complex and context dependent with regard to intercellular adhesion as well as cell spreading. For instance, in human colon endothelial cells, IGF-1R signalling tends to reduce cell–cell adhesion through increased tyrosine phosphorylation of E-cadherin and catenins. Under specific conditions, however, IGF-1R may enhance cell–cell adhesion (Bähr & Groner, 2005).

Disruption of adherens junctions and activation of the MAP kinases is also an outcome of IGF-1R signalling for migratory responses. Activation of the receptor leads to the upregulation of another common angiogenic factor, namely, vascular endothelial growth factor (VEGF), that typically triggers proliferation and chemotaxis of endothelial cells. In pancreatic cancer cells, the activation of IGF-1R upregulates VEGF expression through promotion of hypoxia-inducible factor-1 alpha (HIF-1 α) nuclear translocation with the consequent increase in angiogenesis. In addition, overexpression of IGF-1R is typically observed in human colon cancer cells, and the expression level has been related to tumor grade and stage advancement (Bähr & Groner, 2005).

1.4 Overexpression of IGF-1R in Colorectal Cancer (CRC)

Carcinoma of the colon and rectum is the third leading malignant tumor in terms of incidence and second-leading cause of death among neoplastic diseases worldwide. According to GLOBOCAN data from the World Health Organization's Cancer Research Institute, there were about 1.93 million new cases and around 940,000 deaths attributed to CRC in 2020. Activation of various intracellular signalling pathways by IGF-1R in the colonic mucosal cells aids importation to progress through cell cycle and apoptosis inhibition. Blocking IGF-1R leads to G1 phase cell cycle arrest and significantly limits CRC cell proliferation, survival, and resistance to treatments using radiation therapy (Zhang et al., 2022).

The overexpression of certain proteins belonging to the inhibitor of apoptosis protein (IAP) family, such as baculoviral IAP repeat-containing protein-7 (BIRC7), also known as Livin or melanoma inhibitor of apoptosis, allows CRC cells to escape such programmed cell death. Both IGF-1R and Livin are promising CRC biomarkers, but their contribution towards the normal colonic mucosa to adenoma and cancer stage has received very little attention in research. High expression of IGF-1R and Livin oncogenes in CRC patients can predict the cancer stages, the possibility of metastasis, and the carcinogenic risks. Particularly, IGF-1R is assumed to play a major role in driving neoplastic initiation and progression through the sequence of colorectal mucosa-polyp-cancer (Zhang et al., 2022).

1.5 Overexpression of IGF-1R in Brest Cancer (BC)

As per the World Health Organization, breast cancer is the most common cancer diagnosed with regard to the female population, and its incidence is the strongest determinant of overall cancer killing. Breast cancer is a complex unit comprising five molecular subtypes based on the expression levels of estrogen receptor, progesterone receptor, Her-2, and Ki67. The overexpression of the insulin-like growth factor 1 receptor in several types of cancer, especially breast cancer, has triggered many investigations to determine it as one of the new-generation anticancer treatment targets. It is noted that 50%–93% cases of breast cancer have detectable IGF-1R expression, but it has been implicated in variable prognostic significance (Ianza et al., 2021; Yan et al., 2015).

Besides showing that it regulates the Estrogen receptor (ER)/ Progesterone receptor (PR) signalling pathway of breast cancer, IGF-1R behavior has been reported to be in both in vitro and in vivo studies. It has been reported that proliferation of cancer cells is stimulated through the action of IGF-1R activated by ER, but instead, it uses activation of IGF-1R without any ER involvement to induce mitogenesis. Triple-negative breast cancer or Z represents a sub-type of breast that does not express ER, PR, and Her-2. Effective molecular targets for therapy of triple-negative breast cancer are currently unavailable. Clustering of data, however, reveals the presence of six TNBC subclasses, such as basal-like II and mesenchymal subtypes, which have been shown to be IGF-1R positive; however, prognostic significance for TNBC remains undefined for IGF-1R (Ianza et al., 2021; Yan et al., 2015).

The studies discussed the signalling crosstalk of Her-2 and IGF-1R and proposed a function for the pathway of IGF-1R in trastuzumab resistance; however, their clinical relevance is not yet exhaustively defined (Yan et al., 2015).

1.6 Structure, regions and binding sites of IGF-1R

Just like the peptides, insulin and IGFs belonging to the same family, the IGF-1R is also structurally 50-85% homologous to insulin receptor (Macháčková et al., 2019) with tyrosine kinase domains, juxta-membrane (JM) domains and C-terminal regions having 84%, 61% and 44% sequence identity respectively (Favelyukis et al., 2001). Members of this family are hetero-tetrameric glycoproteins (Favelyukis et al., 2001) with two N-terminal α and C-terminal β subunits, bound by several disulphide bonds forming two $\alpha\beta$ homodimers (Macháčková et al., 2019; Whittaker et al., 2001). Due to high homology with IR, it can be understood that unbound extracellular region of IGF-1R is a Λ -shaped structure which was determined in IR by X-ray crystallography (Cai et al., 2022).

Starting from the N-terminal end, comprise a first leucine rich repeat domain or L1, a cysteine-rich domain or CR, a second leucine rich repeat domain or L2, and the first, second, and third fibronectin III domains- FnIII-1, FnIII-2, and FnIII-3. The seventh domain, known as the insert domain (ID), has an unsolved structure which can be found enclosed in the region of FnIII-2 including the CC' loop that also contains the furin cleavage site, in α/β strand motif (Belfiore et al., 2017).

The "head" of the receptor due to the L1-CR-L2 group of a monomer and "stalk" containing the FnIII-1- FnIII-2-FnIII-3 group of another monomer fall parallel to each other leading to the presence of a fold which two folds of symmetry with an L-shaped configuration. A part of the α chain of ID (a segment called α CT) that is far distal from the N terminus adopts an α helical structure that is situated above the central β sheet (L1- β 2) contained within the L1 domain (Belfiore et al., 2017).

Biophysical and molecular studies have further established that each insulin receptor (IR) monomer consists of two particular insulin binding sites - the first and the secondary. The former is composed of the L1 domain and the α CT' structural element, and their interaction is of the essence for attaching insulin molecule on the receptor as well as its activation. An L1 domain alanine scanning experiment has shown that residues at the β -sheet surface within the L1 domain play a key role in insulin-IR interaction and a number of these also bind α CT'. This indicates that site-1 is established by joint efforts of both protomers, where L1 adhering to α CT' construct encompasses the insulin binding region (Yunn et al., 2023).

Moreover, site-2' situated at the β -sheet region of FnIII-I apparently also help in binding insulin yet is considered a different entity that may also engage insulin independent of site-1. In the

full holo-IR dimer, the two chains are aligned in antipodal orientation with respect to one another. Site-1 and site-2' are present on one face of the dimer, while, on the opposite side, site-1' and site-2 are localized. Also, due to the parallel acquisition of the structures, site 1 and site 2' (site 1' and site 2 as well) on each side are brought into direct contact with each other (Yunn et al., 2023).

1.7 Overview of IR activation

Single insulin receptor with a bound insulin molecule viewed by cryo-EM revealed that binding asymmetry with insulin at site-1 forms asymmetric Γ-shaped structure. With the site-1 L1, CR, L2 and FnIII-1 domains constructing an "elevated head" in one protomer, the same domains in the second protomer construct a "lowered head". The stalk regions which comprise of FnIII-1, FnIII-2 and FnIII-3 remained in both protomers (Yunn et al., 2023).

Activation involves insulin binding to L1 and α CT' at site-1 both at the same time thus leaving the distal side in the receptor unbound. This binding brings forward L1 and α CT' to FnIII-1' more than it is shown with the unbound receptor case. Therefore, the bending involves decreasing the distance between the membrane-proximal ends of FnIII-3 and FnIII-3' since the two stalks are at a closer longitudinal distance. An important feature of this activation is the alteration in the form of α CT- α CT' bridge known to be a disulfide bonded construct. Hence when one α CT moves up, the sister CT moves down, caused by the association of those in between. Now this movement will lead to FnIII-3 ends to get close, bringing into line transmembrane helices and the cytoplasmic kinase domains, helping in the transautophosphorylation for the tyrosine kinase enzyme activity and initiating the downstream signal transduction (Yunn et al., 2023).

1.8 Hypothesized IGF-1R activation

Due to high homology present between IR and IGF-1R and also between insulin and IGF II, it can be hypothesised that the binding mechanism of IGF II with IGF-1R is very similar to that of insulin with IR wherein IGF 2 binds to site 1 initially leading to conformational changes in structure of receptor from Λ -shaped structure to asymmetric Γ -shaped structures. Once the IGF II is bound to site 1, the conformational changes lead to changes in the disulphide bond orientation present between $\alpha CT - \alpha CT'$ bridge, thus bringing the stalks of the receptor closer to each other. Thereby, bringing the transmembrane helices and kinase domains in close proximity and starting the downstream signalling cascade.

However, from a structural point of view, it has been assumed that the site 2' is the only insulin binding site as the site 2' interface of the FnIII 1' in Λ -shaped structure is completely exposed (Yunn et al., 2023).

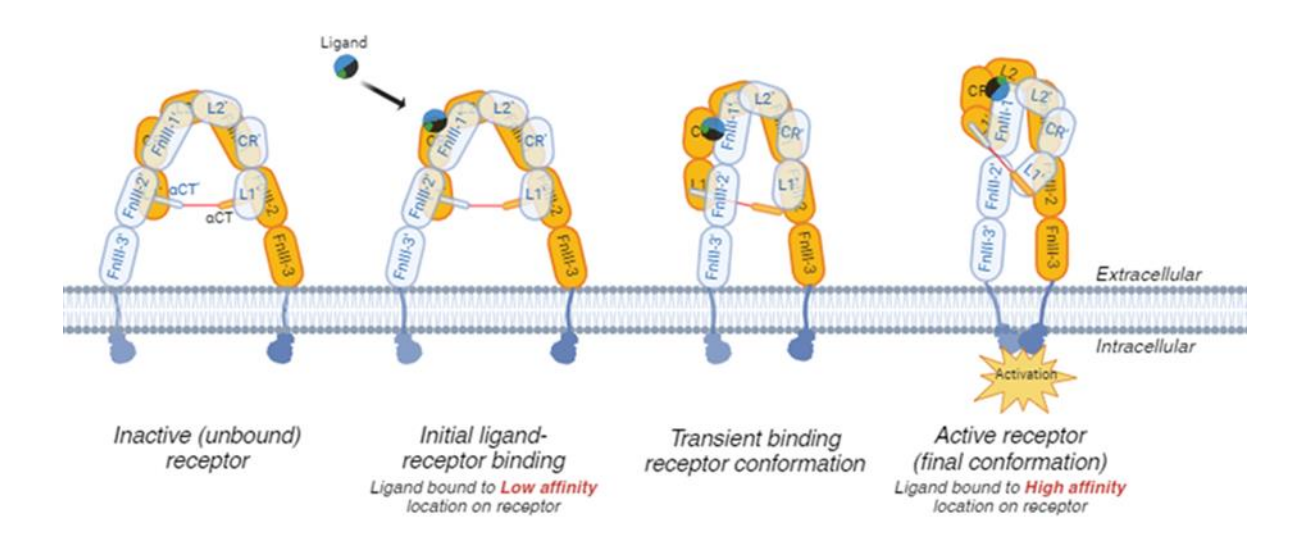


Figure 1:Schematic representation of the stepwise ligand-induced activation of the IGF-1 receptor (IGF-1R).

Figure 1.2: Schematic representation of the stepwise ligand-induced activation of the IGF-1 receptor (IGF-1R). The figure illustrates four conformational states of the IGF-1R dimer during ligand binding and activation. In the inactive (unbound) state, the receptor extracellular domains are extended and separated. Upon ligand approach, it initially binds to a low-affinity site on the receptor, inducing partial rearrangement. This leads to a transient receptor conformation where domain interactions begin to realign. Finally, the ligand engages the high-affinity binding site, inducing a compact and fully active receptor conformation. This facilitates receptor dimerization and downstream intracellular signalling activation.

Domain components such as L1, CR, L2, and FnIII modules are labelled, and αCT segments contribute to conformational rearrangements critical for activation.

Research Gap

The site 2 of insulin receptor involves basic residues like Arg479, Lys484, Leu486, Arg488, Pro537, Leu552 and Arg554 which participate in the interaction with insulin while forming a bond. The two mutants K484E and L552A demonstrated the most significant defects by structural mutagenesis. In contrast to many other tested IR double mutants, the site 2 mutant K484E/L552A strongly fails to activate an insulin-dependent activation in a dose-response assay after exposure to a wide range of insulin concentrations (Uchikawa et al., 2019).

Similarly, on the site 2 of IGF-1R, Arg474, Leu537, His539, Ile476, Thr478, Ser471 residues are found to be equivalent to the site 2 residues in IR involved in binding of IGF II (Xu et al., 2020).

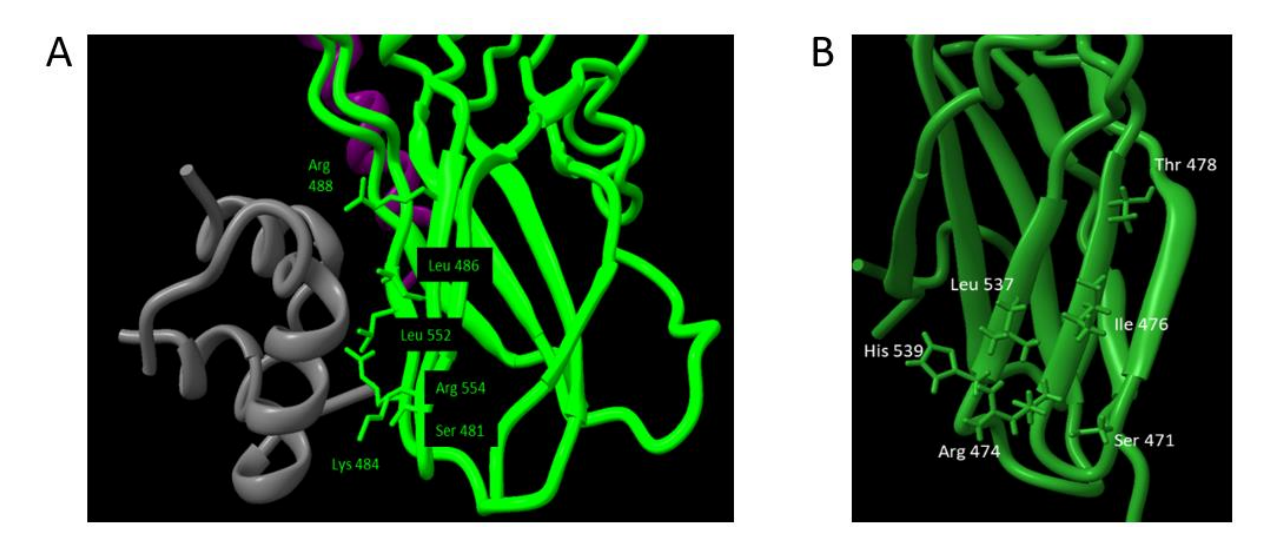


Figure 1.3: Structural visualization of key residues within the IGF-1R receptor involved in receptor-ligand interactions and putative site-2 interface. A) Structural model showing the interaction interface between IGF-1R (green) and an interacting loop (grey). Key residues implicated in ligand or interdomain interactions are highlighted, including Ser481, Arg488, Lys484, Leu486, Leu552, and Arg554. These residues form part of the β-sheet and adjacent loops potentially contributing to the site-2 binding region. B) Close-up view of residues on IGF-1R β-sheet region, including Ser471, Ile476, Thr478, Arg474, Leu537, and His539, which form a structurally conserved surface patch. These residues are candidate sites for mutagenesis to evaluate their role in IGF-1R functional activation and downstream signaling. Structural representations were generated using molecular modeling software, highlighting the spatial arrangement of side chains within the receptor domain.

Table 1.1: Table of corresponding amino acid residues between the insulin receptor (IR) and IGF-1 receptor (IGF-1R) involved in receptor activation and ligand binding.

IR residues	IGF-1R residues
Arg 488	Thr 478
Leu 552	Leu 537
Arg 554	His 539
Lys 484	Arg 474
Leu 486	Ile 476
Ser 481	Ser 471

The listed residues from IR and IGF-1R share conserved or functionally analogous positions in their respective structures. These residues are located within regions critical for receptor dimerization, ligand interaction, or structural stability during the activation process. Residues such as Arg488 (IR) and Thr478 (IGF-1R), and Leu552 (IR) and Leu537 (IGF-1R) are examples of conserved or substituted positions studied for their roles in receptor signaling mechanisms.

However, from past researches, it is still not known yet which residues are significant for the binding of IGF II to site 2 of IGF-1R as the researchers weren't able to capture IGF II bound to site 2 of IGF-1R. This forms the basis of my research to investigate Arg474, Leu537, His539, Ile476, Thr478, Ser471 residues for their significance in having an effect in binding affinity of IGF II at site 2 of IGF-1R since its equivalent residues in site 2 of IR have some effects on binding affinity of IGF II. Thus, by determining the amino acid residues present on the site 2 of IGF-1R, we can develop anti-cancer drugs which can inhibit the binding of the ligand to receptor thereby, mitigating the overexpression effect of the receptor and presenting new therapeutics for cancer treatment.

1.9 Study hypotheses and aims

At present, there is basic understanding regarding the binding mechanism of the insulin and IGFs with their receptors, IR and IGF-1R among researchers by comparing the approach and methods used for studying the binding mechanism of IGFs with IGF-1R to insulin with IR due to their high homology. Despite the fact that, high affinity binding site of IGF-1R is broadly studied regarding its binding efficacy with IGFs, low affinity binding site of IGF-1R remain unexplored. This is due to the fact that, researchers were not able to structurally capture the

IGFs bound to low affinity binding site of IGF-1R leading to utilization of site directed mutagenesis to determine the initial binding site. Hence, the general objective of my research project was to identify specific residues and structure responsible for the initial binding of IGFs to IGF-1R at low affinity binding site.

1.9.1 Study Hypotheses

Hypothesis 1: The interaction of IGFs on FnIII-I domain on IGF-1R is important for the binding of the ligand at low affinity binding site of the receptor.

Hypothesis 2: A key interaction within the high affinity binding site of the IGF-1R involves residue K530 within the FnIII-I domain.

1.9.2 Aims

Aim 1 To investigate the role of IGF-1R residues Ser471, Ile476, Thr478 and their involvement in the low affinity site interaction.

Aim 2: To investigate the role of IGF-1R residue Lys530 in high affinity binding site and interaction with IGFs.

CHAPTER 2: MATERIALS AND METHODS

2.1 Materials

Materials used in this project were of analytical grade, prepared and used in ultrapure water (Elga Chorus), or ultrapure water sterilised at 121°C/17 psi where necessary. Solutions were filtered where appropriate using syringes (Becton Dickinson and Company) with filters of 0.22µM or 0.45µM pore size (Sartorius Mini Start).

2.1.1 DNA Cloning and molecular biology

2.1.1.1 Reagents

Deoxyadenosine phosphate (dATPs), deoxyribonucleotide triphosphate (dNTPs), Taq DNA polymerase, 10x Thermopol buffer, T4 DNA ligase, 10x T4 DNA ligase buffer, restriction enzymes (XhoI, KpnI-HF), 10x rCutSmart buffer, 1kb plus DNA ladder and 6x DNA load dye were purchased from New England Biolabs (NEB). Ampicillin, agar, glycerol, agarose, Tris-Ultrapure, boric acid and bromophenol blue were purchased from Sigma-Aldrich (Merck). pGEM T-easy vector kit was purchased from Promega. MI3F and SP6 primers were purchased from Macrogen. IGF-IR fwd 404v2 and IGF-IR rev seq 519 primer and cDNA g-blocks were designed in-house, then synthesised by Integrated DNA technologies. Sodium chloride (NaCl) was purchased from ChemSupply. Oxoid tryptone was purchased from ThermoFisher. Bacto yeast extract was purchased from Becton Dickinson and Company. QIAprep Spin Miniprep Kit, QIAquick Gel Extraction Kit and QIAGEN Plasmid Midi Kit were purchased from OIAGEN.

2.1.1.2 cDNA

G-block DNA gene fragments were designed by A. Merriman (Forbes' lab), and purchased from Integrated DNA technologies.

Table 2.1: cDNA sequences of designed IGF-1R analogues. The restriction enzymes used in the g-block design have been highlighted (Nsil/Xhol/Kpnl), while the specific codon mutation for each analogue has been highlighted in yellow.

DNA fragment	Sequence (5'-3')			
S471A	TTTTTCTCGAGGCCAACTACAGCTTCTACGTGCTGGACAACC			
IGF-1R	AGAACCTGCAGCAGCTGTGGGACTGGGACCACAGAAACCTG			
Ser471Ala	ACCATCAAGGCCGGCAAGATGTACTTCGCCTTCAACCCCAAG			
	TGTGCGTGTCCGAGATCTACAGAATGGAAGAAGTGACCGGC			
	CCAAGGCAGACAGAGCAAGGGCGACATCAACACCAGAAA			
	CAACGGCGAGAGCCAGCTGCGAGAGCGACGTGCTGCACT			
	TCACCAGCACCACCGCCACCGCCAAGAACAGAATCATCACCT			
	GGCACAGATACAGACCCCCCGACTACAGGGACCTGATCAGCT			
	TCACCGTGTACTACAAAGAGGCCCCCTTCAAGAACGTGACCG			
	AGTACGACGGCCAGG <mark>ATGCAT</mark> GCGGCAGCAACAGCTGGAAC			
	ATGGTGGACGTGGACCTGCCCCCAACAAGGACGTGGAACCC			
	GGCATCCTGCACGGCCTGAAGCCCTGGACCCAGTACGCC			
	GTGTACGTGAAGGCCGTGACCCTGACCATGGTGGAAAACGAC			
	CATCAGGGGCCCAAGAGCGAGATCCTGTACATCAGGAC			
	CAACGCCTC <mark>GGTACC</mark> TTTTT			
I476A	TTTTTCTCGAGGGCAACTACAGCTTCTACGTGCTGGACAACC			
IGF-1R	AGAACCTGCAGCAGCTGTGGGACTGGGACCACAGAAACCTG			
Ile476Ala	ACCATCAAGGCCGGCAAGATGTACTTCGCCTTCAACCCCAAG			
	CTGTGCGTGTCCGAGATCTACAGAATGGAAGAAGTGACCGGC			
	ACCAAGGGCAGACAGAGCAAGGGCGACATCAACACCAGAAA			
	CAACGGCGAGAGCCAGCTGCGAGAGCGACGTGCTGCACT			
	TCACCAGCACCACCAGCAAGAACAGAATCGCCATCACC			
	TGGCACAGATACAGACCCCCCGACTACAGGGACCTGATCAGC			
	TTCACCGTGTACTACAAAGAGGCCCCCTTCAAGAACGTGACC			
	GAGTACGACGGCCAGG <mark>ATGCAT</mark> GCGGCAGCAACAGCTGGAA			
	CATGGTGGACGTGGACCTGCCCCCAACAAGGACGTGGAACC			
	CGGCATCCTGCACGGCCTGAAGCCCTGGACCCAGTACGC			
	CGTGTACGTGAAGGCCGTGACCCTGACCATGGTGGAAAACGA			

	CCACATCAGGGGCGCCAAGAGCGAGATCCTGTACATCAGGA				
	CCAACGCCTC <mark>GGTACC</mark> TTTTT				
T478A	TTTTTCTCGAGGGCAACTACAGCTTCTACGTGCTGGACAACC				
IGF-1R	AGAACCTGCAGCAGCTGTGGGACTGGGACCACAGAAACCTG				
Thr478A	ACCATCAAGGCCGGCAAGATGTACTTCGCCTTCAACCCCAAG				
	CTGTGCGTGTCCGAGATCTACAGAATGGAAGAAGTGACCGGC				
	ACCAAGGGCAGACAGAGCAAGGGCACATCAACACCAGAAA				
	CAACGGCGAGAGCCAGCTGCGAGAGCGACGTGCTGCACT				
	TCACCAGCACCACCAGCAAGAACAGAATCATCATCGCCT				
	GGCACAGATACAGACCCCCCGACTACAGGGACCTGATCAGCT				
	TCACCGTGTACTACAAAGAGGCCCCCTTCAAGAACGTGACCG				
	AGTACGACGGCCAGG <mark>ATGCAT</mark> GCGGCAGCAACAGCTGGAAC				
	ATGGTGGACGTGGACCTGCCCCCAACAAGGACGTGGAACCC				
	GGCATCCTGCACGGCCTGAAGCCCTGGACCCAGTACGCC				
	GTGTACGTGAAGGCCGTGACCCTGACCATGGTGGAAAACGAC				
	CACATCAGGGCCCCAAGAGCGAGATCCTGTACATCAGGAC				
	CAACGCCTC <mark>GGTAC</mark> TTTTT				
K530A	TTTTTCTCGAGGGCAACTACAGCTTCTACGTGCTGGACAACC				
IGF-1R	AGAACCTGCAGCAGCTGTGGGACCTGGGACCACAGAAACCTG				
Lys530Ala	ACCATCAAGGCCGGCAAGATGTACTTCGCCTTCAACCCCAAG				
	CTGTGCGTGTCCGAGATCTACAGAATGGAAGAAGTGACCGGC				
	ACCAAGGCAGACAGAGCAAGGGCGACATCAACACCAGAAA				
	CAACGGCGAGAGCCAGCTGCGAGAGCGACGTGCTGCACT				
	TCACCAGCACCACCAGCAAGAACAGAATCATCACCT				
	GGCACAGATACAGACCCCCCGACTACAGGGACCTGATCAGCT				
	TCACCGTGTACTACAAAGAGGCCCCCTTCAAGAACGTGACCG				
	AGTACGACGGCCAGG <mark>AAGCAT</mark> GCGGCAGCAACAGCTGGAAC				
	ATGGTGGACGTGGACCTGCCCCCAACGCCGACGTGGAACC				
	CGGCATCCTGCACGGCCTGAAGCCCTGGACCCAGTACGC				
	CGTGTACGTGAAGGCCGTGACCCTGACCATGGTGGAAAACGA				
	CCACATCAGGGGCGCCAAGAGCGAGATCCTGTACATCAGGA				
	CCAACGCCTC <mark>GGTACC</mark> TTTTT				

2.1.1.3 Primers

Table 2.2: Summary of primers used for molecular biology components of this study.

Primer name	Sequence	Forward	Product
		or	size
		reverse	
SP6 primer	5' ATTTAGGTGACACTATAG 3'	Reverse	200bp
M13F primer	5' GTAAAACGACGGCCAGT 3'	Forward	1
IGF-IR fwd 404v2	5' AAGAACCTGAGACTGATCCTGGGC 3'	Forward	-
IGF-IR rev seq 519	5'GGGTTCCACTTCACGATCAGCTGGC 3'	Reverse	-

2.1.1.4 Constructs

The hIGF-1R gene construct that was used for this project was previously designed by the Forbes lab (Ms C. Delaine, Prof. B. Forbes) and was codon-optimised (with an unchanged amino acid sequence) for the expression of restriction enzyme sites for cloning and processing. The full-length hIGF-1R has previously been cloned into pcDNA3.1 vector at the HindIII/XbaI sites.

2.1.1.5 Vectors

Table 2.3: Summary of vectors utilised for this study.

Vector name	Antibiotic resistance	Selection	Supplier
pcDNA3.1 (+) vector	Ampicillin	Geneticin	Life Technologies Australia
p-GEM-T Easy vector	Ampicillin	N/A	Promega Australia

2.1.1.6 Bacterial strains

Table 2.4: Summary of bacterial strains utilised for this study.

Bacterial strain	Genotype
Escherichia coli (E.coli) DH5α	F- φ 80lacZ Δ M15 Δ (lacZYA-argF)U169
	$rec A1 end A1 hsd R17 (r_{K} \ , m_{K\text{+}}) pho A$
	supE44 λ ⁻ thi-1 gyrA96 relA1

2.1.1.7 Buffers and Solutions

Table 2.5: Summary table for the list of buffers and solutions with their composition

Solutions and Buffers	Composition		
10x SB buffer	190mM Boric acid and 68mM NaCl in		
	ultrapure water		
0.8% agarose	0.8% (w/v) agarose, 1x SB buffer in		
	ultrapure water		
2% agarose	2% (w/v) agarose, 1x SB buffer in ultrapure		
	water		
3x GelRed staining solution	1:1000 dilution of 10,000x stock GelRed		
	and 0.1M NaCl in ultrapure water		
Luria Bertani (LB) agar	1% (w/v) Tryptone, 0.5% (w/v) yeast		
	extract, 0.5% (w/v) NaCl and 1.5% agar in		
	ultrapure water		
Luria Bertani (LB) Media	1% (w/v) Tryptone, 0.5% (w/v) yeast extract		
	and 0.5% (w/v) NaCl in ultrapure water		
6x DNA load dye	30% (v/v) glycerol, 0.25% (w/v)		
	Bromophenol blue and 0.25% (w/v) Xylene		
	Cyanol in ultrapure water		

2.1.2 Protein expression and quantification

2.1.2.1 Cell culture, transfection and protein quantification reagents

Dulbecco's Modified Eagle Medium (DMEM) and trypsin were purchased from Gibco. Penicillin-Streptomycin (10,000 U/mL) (Penstrep), Lipofectamine 3000 reagent kit and dithiothreitol (DTT) were purchased from ThermoFisher. Dimethyl sulfoxide (DMSO), Coomassie brilliant blue R-250 dye, sodium dodecyl sulfate (SDS), Tween 20, potassium

dihydrogen phosphate (Na₂HPO₄), glycine, N,N,N',N' -Tetramethylethylenediamine (TEMED), ammonium persulfate (APS), foetal bovine serum (FBS), propan-2-ol, hydrochloric acid (HCl), sodium azide and bovine serum albumin (BSA), were acquired from Sigma-Aldrich (Merck). Ethanol, acetic acid and methanol were obtained from ChemSupply. Precision Plus Dual Xtra Prestained Protein Standards, 40% acrylamide and 2% bis-acrylamide were purchased from Bio-Rad. Potassium chloride (KCl) was purchased from Univar. Potassium dihydrogen phosphate (KH₂PO₄) was purchased from JT Baker.

2.1.2.2 Cell lines

A human embryonic kidney 293FT cell line with a targeted knockout of the IR and IGF-1R gene was utilised for this project. The IR/IGF-1R double knockout cells (hereafter denoted "DKO cells") were a kind gift of A/Prof E. Choi, University of Texas Southwestern Medical Center.

2.1.2.3 Antibodies

Primary antibodies used in this study were utilised at a 1:1000 dilution. Secondary antibodies used in this study were utilised at a 1:100,000 dilution.

Table 2.6: Summary of IGF-1R, IR, and cell signalling molecule antibodies used in this study.

Antibody	Supplier/	Type	Clonality	Host	Epitope
	Product no.				
IGF-1R β	Cell	Primary	Polyclonal	Rabbit	hIGF-1R β carboxy-
unit	Signalling				terminal residues
	(#3027)				
Phospho-	Cell	Primary	Monoclonal	Rabbit	hIGF-1R β residues
IGF-1R β	Signalling				Y1135/Y1136
	(#3024)				
Goat anti-	Invitrogen	Secondary	Polyclonal	Goat	Rabbit gamma
rabbit IgG	800				immunoglobulins

2.1.2.4 Buffers and Solutions

 Table 2.7: Summary table for the list of buffers and solution with their composition

Buffers and Solutions	Composition
Complete media	10% (v/v) FBS, 1% (v/v) Penstrep (100U/mL
	of penicillin, 100µg/mL streptomycin), 6mM
	Glutamax in DMEM with sodium carbonate
Blocking buffer	5% BSA in 1x TBST
Western transfer buffer (WTB)	249nM glycine, 24mM Tris-Ultrapure and
	20% (v/v) methanol in ultrapure water
10x Tris-buffered saline (TBS)	1.5M NaCl and 250mM Tris-Ultrapure in
	ultrapure water
1x TBST	1x TBS and 0.1% (v/v) Tween-20 in
	ultrapure water
10x Glycine-tris SDS buffer (GTS)	1.92mM glycine, 250mM Tris-Ultrapure and
	0.1% (v/v) SDS in ultrapure water
10x Phosphate-buffered saline (PBS)	1.37M NaCl, 27mM KCl, 20mM KH ₂ PO ₄
	anhydrous and 100mM Na ₂ HPO ₄ in
	ultrapure water
Trypsin solution	1x trypsin in 1x PBS buffer
Gel fixer solution	40% (v/v) ethanol and 10% (v/v) acetic acid
	in ultrapure water
Coomassie blue staining solution	0.1% (v/v) Coomassie Brilliant Blue R-250
	dye, 40% (v/v) ethanol and 10% (v/v) acetic
	acid in ultrapure water
Gel destain solution	10% (v/v) acetic acid in ultrapure water
5x protein load dye (pre-prepared by	10% (v/v) sodium dodecyl sulfate (SDS),
laboratory)	250mM Tris-Ultrapure pH 7, 0.02% (v/v)
	bromophenol blue and 50% (v/v) glycerol in
	ultrapure water
	1
Lower buffer	1.5M Tris-Ultrapure and 0.4% (v/v) SDS in
Lower buffer	1.5M Tris-Ultrapure and 0.4% (v/v) SDS in ultrapure water, pH to 8.8
Lower buffer Upper buffer	• • • • • • • • • • • • • • • • • • • •

4% Tris-glycine Laemmli stacking gel	3.8% (v/v) acrylamide, 0.1% (v/v) bis-	
	acrylamide, 25% (v/v) upper buffer, 0.1%	
	(v/v) TEMED and 0.1% (w/v) ammonium	
	persulfate (APS), in ultrapure water	
10% Tris-glycine Laemmli separating gel	9.7% (v/v) acrylamide, 0.3% (v/v) bis-	
	acrylamide, 25% (v/v) lower buffer, 0.1%	
	(v/v) TEMED and 0.1% (w/v) APS, in	
	ultrapure water	

2.2 Methods:

2.2.1 Bacterial cloning

The methods mentioned for bacterial cloning have been troubleshot and optimized by me by changing several factors affecting the protocols such as concentration of T4 ligase, using a new pGEM-T easy kit, insert:vector ratio for ligations, using new batch of competent DH5 α cells and using log-wave UV box instead of using ChemiDoc Imaging System for excision of bands in agarose gels. However, due to interest of time I had to move on from bacterial cloning to cell culturing and A. Merriman helped me generating the cloned expression vector mutants using the optimized conditions established.

2.2.1.1 Poly A-tailing of g-blocks:

Four G-blocks were purchased to enable construction of 4 mutant receptor clones (S471A IGF-1R, I476A IGF-1R, T478A IGF-1R and K530A IGF-1R). Poly-A tailing of 100ng of G-blocks was performed as per Taq DNA polymerase protocols (NEB). For 50µL of poly-A tailing of G-blocks of DNA, 1mM of dATPs, 1X thermopol buffer and 1.25 units of Taq polymerase in ultrapure water was added in an Eppendorf tube and incubated at 37°C for 30 minutes and using at 72°C for another 30 minutes. The poly-A tailing of the G-block inserts were completed by A. Merriman.

2.2.1.2 Ligation of G-blocks into pGEM-T easy vector:

Poly-A tailed G-blocks were then ligated into linear pGEM-T easy cloning vector according to manufacturer's protocols (NEB). For ligation of 62ng of inserts in 10 μ L reaction, 12.5ng of vector, 1X ligation buffer and 1.5 Weiss units of T4 DNA ligase was added in ultrapure water, kept for incubation at room temperature for 1 hour and then stored at 4°C overnight before moving on with transformation into competent DH5 α cells (previously prepared by M. Fitzgerald). For transformation of pGEM-t easy ligation samples, 100 μ L of DH5 α cells were thawed on ice before transforming it with 5 μ L of ligated vector samples and mixed by flicking the mixture. The DH5 α cell mixture was incubated on ice for 15 mins, heat-shocked for 2 mins at 42°C and again incubated on ice for 5 mins. 800 μ L of room temperature LB broth was added before incubating the cell mixture at 37°C for 20 minutes. The cell mixture was centrifuged in a table-top centrifuge at 2000 rpm for 2 mins. 800 μ L of supernatant was discarded and resuspended the pellet in rest of the supernatant before pipetting 100 μ L of this transformed cell mixture into a LB+ Ampicillin plate and incubated it for overnight at 37°C.

Ligation of S471A, I476A and T478A analogues was completed by A. Merriman.

2.2.1.3 Colony PCR screening for successful ligation colonies:

Colony PCR was performed as a confirmatory procedure for successful ligation of pGEM-T easy vector with G-block inserts according to manufacturer's protocol for Taq polymerase and thermopol buffer (NEB). Post transformation of pGEM-T easy ligation samples into DH5a cells, a single colony was picked and swirled in 50µL ultrapure water in an Eppendorf tube which was then streaked on LB+ Ampicillin agar plate. To prepare template DNA, cell sample in 50µL was boiled at 95°C for 5 mins. To prepare a colony PCR sample, 30µL of mastermix containing 1x Thermopol buffer, 0.2mM dNTPs, 0.2µM of SP6 primer and M13F primer and 2 units of Taq polymerase in ultrapure water and 20μL of boiled template DNA sample. The PCR reaction was carried out in Thermocycler for 30 cycles of 95°C for 30 seconds, 55°C for 45 seconds and 68°C for 55 seconds and a final extension in the end. Agarose gel electrophoresis of the colony PCR product was conducted by adding 4µL of amplified DNA to 2μL of 6x Load Dye and was ran on a 2% agarose gel in 1X SB buffer at 100V for 35 minutes. The gel was then stained with Gel Red for 5 minutes and was visualised using ChemiDoc Imaging System on a UV/Blot tray. The successful ligation of G-block inserts with pGEM-T easy vector showed bands at around 500bp marker size and these samples were then selected for further procedures.

Successful ligation S471A, I476A, T478A and K530A was previously screened by A, Merriman

2.2.1.4 Miniprep of successful Colony PCR samples:

Miniprep of successfully ligated pGEM-T easy+ IGF-1R mutants was performed using QIAprep Miniprep Kit. In short, a single colony of the successful samples was picked from the Colony PCR stock plate and was inoculated in conical flask containing 5mL pre-warmed LB media with 100μg/mL Ampicillin which was then incubated with agitation at 37°C overnight for 12-16 hours. This culture was then centrifuged at 6800x g for 3 mins in a Multifuge. pGEM-T easy vector + IGF-1R mutants were purified from the pelleted cells using the QIAprep Spin Miniprep Kit and following manufacturer's protocols. The purified vector complex was then eluted and resuspended in 10mM TrisCl, pH 8.5 and quantified their concentration using Nanodrop. The purified vector was then electrophoresed to determine its purity in 2% agarose in 1X SB buffer at 100V for 50 mins, stained with Gel Red and visualised using ChemiDoc Imaging System as described in section 2.2.1.3

2.2.1.5 Double Restriction Digestion of pGEM-T easy vector+ IGF-1R mutants with XhoI/ KpnI-HF and its gel extraction:

The purified vector complex was subjected to double restriction digestion by XhoI and KpnI-HF to cut out the IGF-1R mutant fragments from the pGEM-T easy vector by following the manufacturer's protocol (NEB). In short, 1µg of purified pGEM-T easy+ IGF-1R mutant plasmids was digested by adding KpnI-HF first and incubated at 37°C for 1 hour. Then, XhoI was added to the mixture and incubated at 37°C overnight to assure complete digestion of the plasmids. The 50µl of digested plasmids were then added to 15µl of 6X Load Dye and electrophoresed in 2% agarose in 1X SB buffer at 100V for 75 mins. The gel was then stained with 3X Gel Red and visualised using ChemiDoc Imaging System as described in section 2.2.1.3. The digested IGF-1R mutant fragments were excised from gel using the gel excision tool. The IGF-1R mutant gene fragments were extracted from the gel using QIAquick gel extraction kit following the manufacturer's protocol and eluted the purified IGF-1R mutant gene fragments in 10mM TriCl, pH 8.5 provided in the kit. To determine the mass of the purified IGF-1R mutant gene fragments, they were electrophoresed as described in section 2.2.1.3 alongside 1kb Plus Molecular Ladder (NEB).

Successful restriction digestion and purification of pGEM-T easy+ IGF-1R mutant fragments of S471A, I476A and T478A were completed by A. Merrriman.

2.2.1.6 Ligation of digested IGF-1R mutant gene fragments with mammalian expression vector pcDNA3.1+ IGF-1R (-XhoI/KpnI-HF):

Isolation of gene fragments of IGF-1R mutant analogues from pGEM- T easy as described in section 2.2.1.5 was carried out and ligated with pcDNA3.1+ IGF-1R (-X/K). After an optimisation of vector:insert molar ratio as per the manufacturer's protocol (NEB), a molar ratio of 8:1 of vector:insert was used along with 1X T4 ligase buffer, 1 unit of T4 Ligase and ultrapure water in a $10\mu L$ reaction. The reaction mixture was incubated at room temperature for 3 hours and then overnight at 4°C. The ligation samples were then transformed as described in section 2.2.1.2. The resultant colonies were cultured overnight for preparing minipreps using the QIAprep Spin Miniprep Kit as described in section 2.2.1.4. The resultant purified positive samples were quantitated for their concentration using a NanodropOne spectrophotometer. A sample of each bacterial culture was kept as a stock which was prepared by adding 250 μ l of cultured bacteria with 80% glycerol in a 1:1 ratio and storage at -80 degrees.

Credits to A. Merriman for successfully producing Alkaline Phosphatase-treated pcDNA3.1+ IGF-1R (-X/K).

Ligation samples of S471A, I476A and T478A was successfully completed by A. Merriman.

2.2.1.7 Confirmatory restriction digestion of expression vector pcDNA3.1+ IGF-1R (-X/K) with mutant gene fragments:

G blocks were originally designed to introduce a new silent restriction enzyme site (NsiI enzyme). To confirm the presence of IGF-1R mutant gene fragments in mammalian expression vector pcDNA3.1+ IGF-1R (-X/K), a small-scale restriction digestion was set up. In a 10μL reaction, 200ng of the ligated vector+ insert sample and 50ng of pcDNA3.1+ IGF-1R (wild type) vector as negative control were digested using NsiI enzyme respectively as described in section 2.2.1.5. After restriction digestion, 4μL of the digested ligation sample was added with 2μL of 6X Load Dye and electrophoresed using a 0.8% agarose gel in 1X SB Buffer at 100V for 1.5 hours. The gel was then stained for 5 mins in 3X Gel Red stain and viewed using a ChemiDoc Imaging System. A sample of 1kb plus Molecular Ladder (Thermofisher) was included on the gel. Successfully ligated samples showed two bands of 3200bp and 400bp, size whereas the unligated samples containing wild type IGF-1R insert showed just one band of 9.5 kb. The positively ligated samples of pcDNA3.1+ IGF-1R (-X/K) with IGF-1R mutant gene fragments were then sent off for Sanger sequencing.

Successful small scale restriction digestion by NsiI of S471A, I476A and T478A was performed by A. Merriman.

2.2.1.8 Sanger Sequencing of pcDNA3.1+ IGF-1R mutant gene fragments:

For Sanger sequencing in a 1.5ml Eppendorf tube, 1µg of purified plasmid, 10pmol each of IGF-1R 404v2 primer and IGF-1R reverse sequence 519 primer was added in ultrapure water up to 12µl. It was sent to Australian Genome Research Facility (Waite Campus) for Sanger sequencing.

2.2.1.9 Midipreps of successfully pcDNA3.1+ IGF-1R (-X/K) with IGF-1R mutant gene fragments:

After confirming the sequence of each construct large scale DNA preparations were made for subsequent expression studies. Cultures of $5\mu L$ of transformed DH5 α cells from glycerol stocks were inoculated into 50mL LB media with $100\mu g/$ mL Ampicillin and incubated for 12-16

hours at 37°C with agitation until the OD at 600nm reached between 2-3. For this midiprep, Thermo Scientific GeneJET Plasmid Midiprep Kit was used and the manufacturer's protocol for plasmid DNA purification for low-speed centrifuge was followed to elute out the plasmid from the cells. The purified plasmid DNA was eluted in 10mM Tris-HCl, pH 8.5 and was later on used to transfect the HEK 293FT Double K/O (-IR/ IGF-1R) cell lines to analyse the expression and activation of the IGF-1R receptors on the cells.

2.2.2 Cell culture and transfection of IGF-1R gene mutants

2.2.2.1 Culturing of Double KO cells and its maintenance:

A human embryonic kidney cell line, HEK 292FT cell line with targeted IR and IGF-1R gene double knock-outs (293FT DKO cells, a kind gift of A/Prof E. Choi, University of Texas Southwestern Medical Center) was maintained in Dulbecco's Modified Eagle Medium (DMEM) with sodium carbonate supplemented with 10% Fetal Bovine Serum (FBS), 1% Penicillin and Streptomycin (Pen/Strep) and 6mM Glutamax. This supplemented DMEM media is the complete media used in this research for culturing the cells. Passaging of cells was done routinely when the confluency used to reach between 75-80%. The cells were passaged by aspirating the media out slowly with vacuum on a low-pressure setting. The cells are then washed with 1X PBS buffer. Once the cells are washed with PBS and the flask is aspirated, then 1X trypsin is added into to flask. The cells were left to incubate at room temperature with trypsin for 3-4 mins and was checked to see if the cells have lifted off from the flask or not. If the cells haven't lifted off, short gentle taps at the edge of the flask were given to accelerate the process of trypsinization. After successful trypsinization, complete media was added into the flask to neutralize the action of trypsin. The cells were then split into new flasks between 1:3 to 1:5 ratio and returned to incubator to incubate at 37°C, 5% CO₂.

2.2.2.2 Determining cell density and viability:

Cell density and its viability were checked after freeze thawing of the cells and also during the transfection of the cells. It was also checked occasionally during the passages. For measuring the cell density and cell viability, $10\mu L$ of the cell suspension was added with $10\mu L$ of trypan blue dye in a sterile 1.5mL Eppendorf tube. Then, $10\mu L$ of this cell and dye mixture was pipetted out and loaded onto a hemocytometer. The cell density was checked by counting the number of live and dead cells present in the squares of the chamber under a compound microscope. The following equation was used to calculate the cell density and cell viability.

Cell Density
$$\left(\frac{cells}{mL}\right) = \frac{Sum\ of\ alive\ cells}{Squares\ counted}x$$
 Dilution factorx 10^4

$$Cell\ Viability = \frac{Sum\ of\ alive\ cells}{Sum\ of\ all\ cells}x\ 100$$

2.2.2.3 Freeze thawing of HEK 293FT Double KO (-IR/IGF-1R) cells:

Frozen DKO cells stored in -80°C were transported on wet ice to thaw the cells. I pipetted out 7mL of the complete media into a 10mL tube (Corning) and 5mL in T-25 flask and kept to warm up in heating beads. To increase the rate of thawing, the cell vial was put in heating beads for 2 mins. Once the media in 10mL tube was had been warmed up, 1mL of media was transferred into the cell vial and gently and slowly mixed with the cell suspension. The cell suspension was then completely transferred into the 10mL tube containing the complete media. The cell suspension was not mixed by pipetting up and down as these cells were very fragile and anymore rough handling of the cells be done, that would affect the viability of the cells. Cell viability and density were determined as mentioned in section 2.2.2.2. The cell suspension in 10mL tube was then centrifuged at 1000 rpm for 2 mins and discarded the supernatant (Megafuge 8R Small Benchtop Centrifuge). The pellet was then re-suspended by transferring the media from T-25 flask into the 10mL tube. The pellet was gently re-suspended with media till no lumps are visible. This cell suspension was transferred back to T-25 flask and incubated at 37°C, 5% CO₂.

2.2.2.4 Transfection of IGF-1R mutants into HEK 293FT Double KO (-IR/IGF-1R) cells:

DKO cells were seeded at a density of 8x10⁵ cells/well into a 6-well plate in 2mL complete media and incubated at 37°C, 5% CO₂ for 24 hours or until it reached confluency of 60-70%. The cells were transfected with Lipofectamine 3000 Reagent Kit (Invitrogen) using the manufacturer's protocol. 2.5μg of Plasmid DNA, 3.75μL of Lipofectamine 3000 Reagent and 5μL of P3000 Reagent was used for per well. The plate was then kept for incubation at 37°C, 5% CO₂ for 24 hours. Lipofectamine 3000 Reagent and P3000 Reagent were mixed in a serum-free and antibiotic-free media as the manufacturer's protocol suggested that formation of lipid complexes would be hindered in media containing serum and antibiotic. However, once the lipid complexes were formed, they could be added to the cells containing complete media.

After 24 hours of transfection, the cells were serum starved of FBS before it is stimulated with IGF-I. Serum starvation caused the cells to come in sync and arrest at G_0/G_1 phase of cell cycle,

thereby stopping the growth and cell metabolism. Additionally, by removing FBS, we also removed insulin and IGF ligands present in the serum responsible for cell growth and metabolism. However, replacing FBS with BSA ensured supplementation of adequate nutrition to the cells in the absence of serum. For serum starvation, complete media was aspirated slowly with low vacuum as there was a high chance of cells lifting off from the plate and replaced with serum- starve media containing 0.5% BSA in DMEM media by adding the serum-starve media slowly into the well along the walls of the well to not disturb the monolayer and incubated at 37°C, 5% CO₂ for 16 hours overnight. Post serum starvation, the cells were stimulated for 10 mins with 10nM IGF-I incorporated in serum-starve media and incubated at 37°C, 5% CO₂.

For each experiment, there were two technical replicates transfected with midi-prepared IGF-1R mutant constructs and WT IGF-1R. Technical replicates transfected with WT IGF-1R DNA were used as a control to determine the regular expression and activation of the receptor when compared with the experimental mutants.

2.2.2.5 Lysis of transfected cells and preparation of lysates for protein quantification:

Post stimulation of transfected cells with 10nM IGF-I for 10 mins, the cells were lysed using the HEPES lysis method previously established in the laboratory. For cell lysis, 0.1% (v/v) protease inhibitor cocktail, one Phospho stop tablet (Roche) per 10mL, 2mM Sodium orthovanadate (Na₃VO₄) and 100mM Sodium flouride (NaF) was added fresh to the HEPES lysis buffer base. The media was then aspirated from the wells at a low vacuum speed and 200µL of the pre-chilled complete HEPES lysis buffer was added to each well and incubated at 4°C for 1 hour by agitating it every 15 mins. The cell lysates were then scraped using a cell scraper and was spun at 13000 rpm for 3 mins at 4°C to remove all the cell debris. The purified cell lysates were then aliquoted for protein quantification and separation and were stored at -80°C freezer. Protein quantification was performed using the Bio-Rad DCTM Protein Assay as per the manufacturer's protocol for microassay plate.

2.2.3 Separation of proteins using SDS PAGE and quantitation of IGF-1R mutant's expression

2.2.3.1 Separation of proteins by SDS-PAGE:

Polyacryalmide gels were made in-house comprising of 10% (v/v) Tris-glycine Laemmli separating gel with 4% (v/v) stacking gel according to manufacturer's protocol (Bio-Rad). 40µg of proteins were loaded in each well after quantifying it using DC assay. Lysate samples

along with Bio-Rad Precision Plus protein marker were electrophoresed using 1x GTS Buffer in ultrapure water at 100V for 60 minutes or until the marker has reached at the end of the gel. Post electrophoresis, the protein gels underwent Western Transfer as explained in section 2.2.3.2.

After Western transfer, the protein gels were stained with R-250 Coomasssie Blue staining solution. For this, the gels were fixed by adding Gel Fixer just to enough to cover the gel for 5 minutes at room temperature on a platform mixer (Ratak). The gels were stained with R-250 Coomassie Blue stain just enough to cover the gel for 1 hour at room temperature on platform mixer before adding the Gel Destain for overnight at room temperature on a platform mixer. The gels were then visualised and imaged using ChemiDoc Imaging System.

2.2.3.2 Western Transfer of proteins onto nitrocellulose membranes:

Post SDS-PAGE Electrophoresis, the separated proteins in gel were transferred onto 0.2μm nitrocellulose membrane with Western transfer methods established in our laboratory. Separated protein samples were transferred at 170mA for 2 hours in a Wet Tank Blotting System (Bio-Rad) with freshly made Western Transfer Buffer (WTB). After Western transfer, the blot membrane was then blocked with blocking buffer comprising of 5% BSA in 20mL 1x TBST for overnight at room temperature on a platform mixer. Addition of blocking buffer ensures blocking of all free sites where protein was unbound to the membrane thereby limiting the no-specific binding of antibodies and reducing the total background signalling. After blocking, the blots were then probed with primary antibodies or was stored in a plastic bag with 1x TBST at 4°C for long-term storage.

2.2.3.3 Probing with antibodies and imaging the blots:

Primary antibodies against specific proteins of interest were diluted 1:1000 in 1xTBST with a total volume of 4mL in a 50mL tube. The blots were added into the tube by carefully folding the blots and avoiding any overlap of blots if possible. The blots were probed with primary antibodies for overnight at 4°C on a tube roller (Ratak). After incubating the blots with primary antibodies for overnight, the blots were washed with 1x TBST for 5 times for 5 minutes each. After a series of washes, the blots were then probed with secondary antibodies which were diluted 1:100000 in 1x TBST in a total volume of 25mL and incubated at room temperature for 1 hour by covering it in foil on a tube roller. Prior to imaging, the blots were washed with 1x TBST for 5 times for 5 minutes each and imaged using ChemiDoc Imaging System. This

wash step is necessary to remove excess secondary antibodies present on the blot as it may interfere by presenting a high background signal while imaging the blot if not removed.

CHAPTER 3: RESULTS

3.1 Cloning of IGF-1R FnIII-I domain mutants and K530A into pcDNA3.1+ IGF-1R mammalian expression vector

3.1.1 Cloning Strategy:

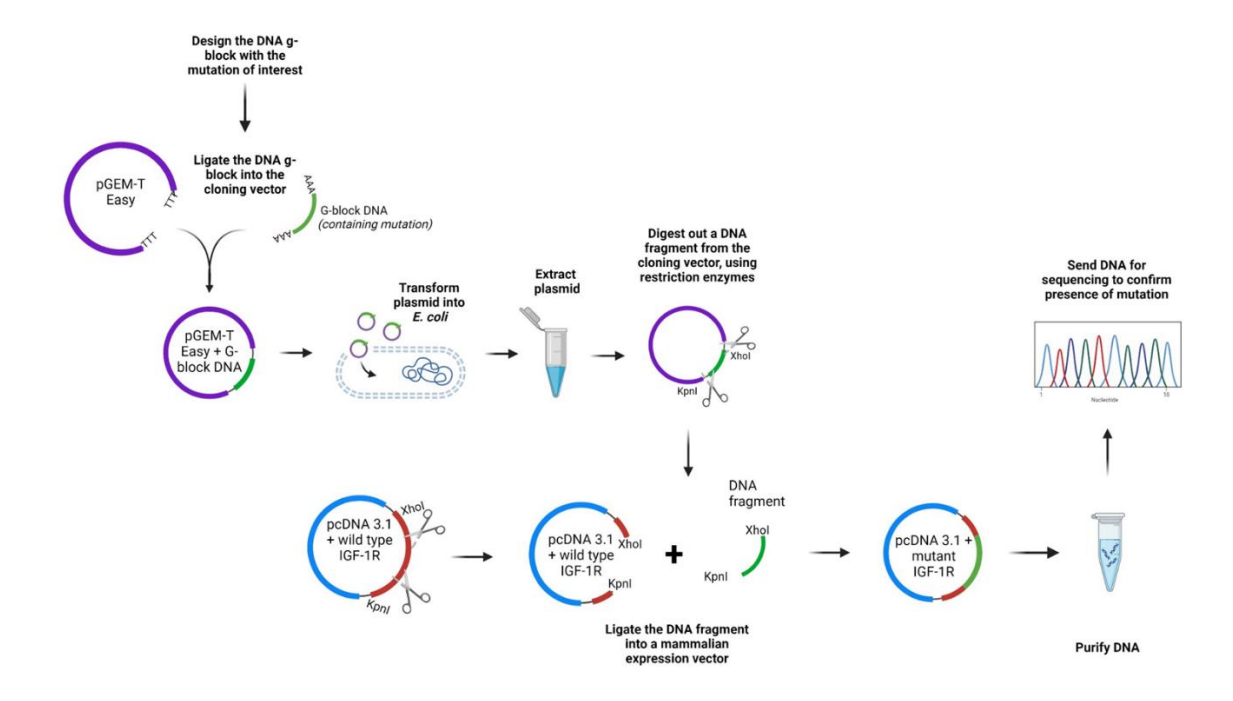


Figure 3.1: Schematic representation of the cloning strategy applied to generate IGF-1R mutant gene fragments. The process of cloning began with designing a synthetic DNA gblock having the mutation of interest. This g-block was then ligated into the pGEM-T easy cloning vector system, which is then transformed into E. coli DH5 α cells. For plasmid extraction, double restriction digestion with XhoI and KpnI-HF restriction enzymes was performed to excise the mutant inserts. The digested mutant inserts were then ligated with digested pcDNA3.1+ IGF-1R cut with same restriction enzymes. The resulting recombinant plasmid is then purified and sequenced to confirm the successful ligation of mutant inserts into the expression vector.

The g-block DNA fragments with specific point mutations in IGF-1R gene sequence were designed by A. Merriman (Forbes Lab) and produced by Integrated DNA Technologies. Four IGF-1R mutants were designed to investigate these aims- Ser471, Ile476, Thr478 and Lys530 was mutated to a non-polar alanine (S471A, I476A, T478A and K530A respectively) These g-

block DNA fragments then underwent various DNA cloning process to produce a final expression plasmid comprising these mutations individually (as described in figure 3.1).

3.1.2 Ligation of designed IGF-1R mutant gene fragments into PGEM-T easy cloning vector:

To commence with the DNA cloning process of the IGF-1R mutant constructs, the designed mutant g-blocks of DNA went through ligation process to ligate into PGEM-T easy cloning vector. For ligation, a ratio of 2:1 of insert: vector was used to successfully ligate the insert into the plasmid vector. To determine the amount of insert and vector that was required for a successful ligation was calculated using the following equation

$$Insert\ DNA\ (ng) = \frac{ng\ of\ vector\ x\ kb\ size\ of\ the\ insert}{kb\ size\ of\ vector}\ x\ insert: vector\ ratio$$

Using the above equation, a ligation reaction was set up as described in section 2.2.1.2. The ligation sample was then transformed into E. coli DH5 α cells by adding 5 μ L of the ligation sample to cells. To confirm successful transformation of the cloning vector into the cells, colony PCR was carried out with M13F and SP6 primers. This amplified sample was then electrophoresed on 2% agarose gel as described in section 2.2.1.3 and checked to confirm successful transformation of mutant insert ligated cloning vector into DH5 α cells.

Table 3.1: Comparison of colony formation under different cloning conditions using the pGEM system. The table shows the number of bacterial colonies observed in the presence or absence of the I476A insert in four experimental conditions: Exp. 1 as use of an old pGEM kit, Exp. 2 as use of new ligase, Exp. 3 as use of a new pGEM kit and Exp. 4 as use of new pGEM kit to long-wave UV light. "NA" indicates data not available. The presence of colonies without insert indicates background vector self-ligation, while colonies with the I476A insert indicate successful ligation and transformation.

		No insert	+ I476A insert	Kit positive
		(colonies)	(colonies)	control
				(colonies)
Experiment 1	Old pGEM kit	92	72	NA
Experiment 2	New ligase	24	21	14
Experiment 3	New pGEM kit	17	19	15
Experiment 4	New pGEM kit	0	152	NA
	+ UV long wave			

However, it was observed at I was not getting a successful transformation of pGEM-T easy vector+ I476A mutant insert even after repeating the transformation process a few times as I kept on getting a high number of colonies for no insert control and low number of colonies for ligated test sample. To address this issue, I optimized and troubleshot the ligation reaction with various control factors such as using a new T4 DNA ligase, a new pGEM-T easy kit or a combination of those as described in Table 3.1. After I optimized the ligation reaction by using a new pGEM-T easy kit with UV long wave, I got successful ligation of I476A mutant insert with pcDNA3.1+ IGF-1R expression vector.

3.1.3 Restriction of digestion of pGEM-T easy + IGF-1R mutant g-block and their gel extraction:

After confirming successful ligation of pGEM-T easy vector with IGF-1R mutant g-blocks, the next step was to isolate the IGF-1R mutant gene fragments from pGEM-T easy vector and prepare it for ligation with pcDNA3.1 mammalian expression vector. For this, the pGEM-T easy cloned vector was digested with XhoI and KpnI-HF as described in section 2.2.1.5. The digested sample was then run a 2% agarose gel and excised using an Xtracta tool (GeneWorks).

Figure 3.2 shows successful restriction digestion of IGF-1R mutant gene fragments from the cloning vector.

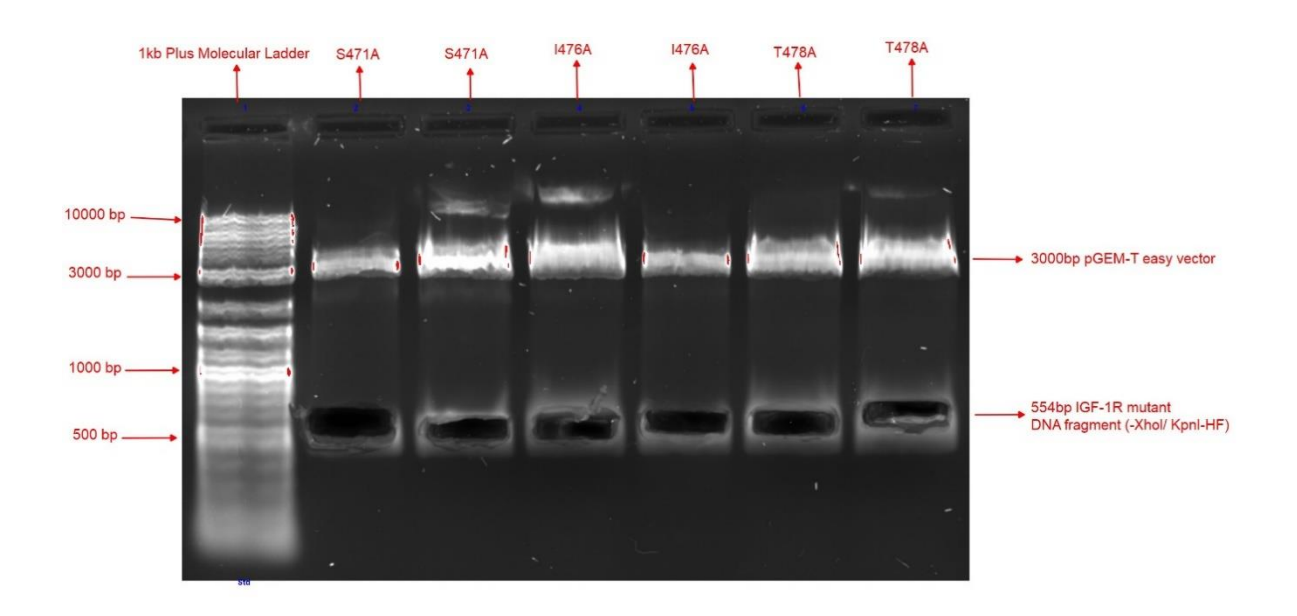


Figure 3.2: Agarose gel electrophoresis of restriction-digested pGEM-T easy vector containing IGF-1R mutant DNA fragments. pGEM-T easy plasmid vector constructs encoding IGF-1R mutants S471A, I476A, and T478A were digested with XhoI and KpnI-HF at 37°C to confirm the presence of the insert. These constructs were run on a 2% agarose in 1x SB buffer at 100V for 1 hour and stained with 3x GelRed stain for 2-5 mins and visualised using ChemiDoc Image System. The bands were excised using the UV long-wave box. Each lane displays two bands corresponding to 3000bp pGEM-T easy vector and the 554bp IGF-1R DNA mutant fragment. A 1kb Plus Molecular Ladder (NEB) was used as the standard. Successful digestion in all mutant constructs confirm proper insertion of the IGF-1R mutant fragments into the vector.

The DNA excised from the gel was then extracted using the gel extraction kit (QIAGEN) and the concentration of purified mutant gene fragments were quantified using Nanodrop as described in section 2.2.1.5. To ligate mutant gene fragments with pcDNA3.1 expression vector, the expression vector was also cut with the same restriction enzymes to produce the same cut sites. Restriction digestion of pcDNA3.1 expression vector was successfully performed as shown in figure.

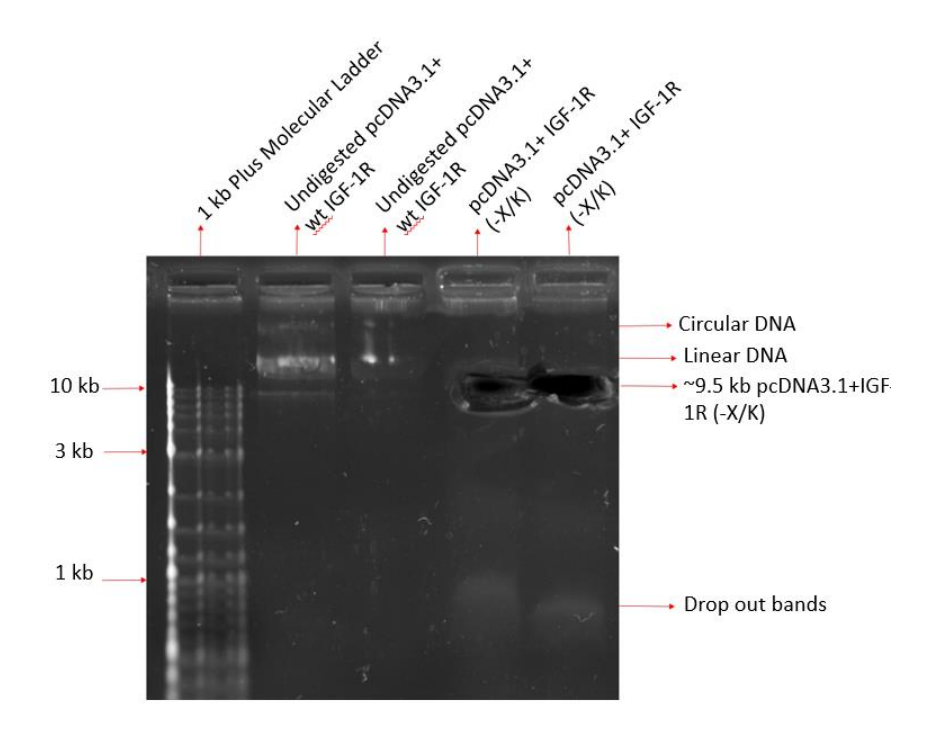


Figure 3.3: Agarose gel electrophoresis showing double restriction digestion of pcDNA3.1+ wt IGF-1R with XhoI and KpnI-HF. pcDNA3.1 expression vector with wild type IGF-1R was double digested with XhoI and KpnI-HF at 37°C, ran on 0.8% agarose gel in 1X SB buffer at 100V for 1.5 hours and stained it with 3X GelRed dye for 2-5 minutes. Lane 1 represents 1kb Plus Molecular Ladder (NEB), Lane 2 and 3 represent undigested pcDNA3.1+ wt IGF-1R vector and Lane 4 and 5 represent double digested pcDNA3.1+ wt IGF-1R (-X/K) vector. The presence of linearised bands of ~9.5kb size in lane 4 and 5 concluded that it was a successful restriction digestion of the expression vector.

3.1.4 Successful ligation of pcDNA3.1 expression vector with IGF-1R mutant inserts:

IGF-1R mutant gene fragments (-X/K) were ligated into pcDNA3.1 + IGF-1R (-X/K) in a ligation reaction by using a ratio of 1:8 of insert:vector. Using the ligation equation stated above in section 3.1.3, mutant gene fragments (-X/K) were ligated to the cut expression vector as detailed in section 2.2.1.6.

Before getting successful ligation samples, I had to troubleshoot and optimize ligation controls as I kept on getting no colonies in 'no insert control' and 'ligation test sample' after transforming it into DH5 α cells. Various factors were tested such as using a new T4 DNA ligase and using different inset:vector ration . However, it was found out that the UV wavelength used in ChemiDoc Imaging System was denaturing the structure of DNA bands present in the gel. Thus, a long-wave UV box was then used to excise the digested DNA bands

in the gel. Post this optimization, I got positive number of colonies in the 'ligation test sample' with no colonies in 'no insert control' transformation.

To confirm the successful ligation of IGF-1R mutant gene inserts into pcDNA3.1 expression vector, a confirmatory restriction digestion was performed as described in section 2.2.1.8 and the ligation samples containing the mutant gene inserts were then sent for sanger sequencing. Figure 3.4 confirms the ligation of IGF-1R mutant inserts- in expression vector due to the presence of 2 bands of 6kb and 3.5kb size post digestion.

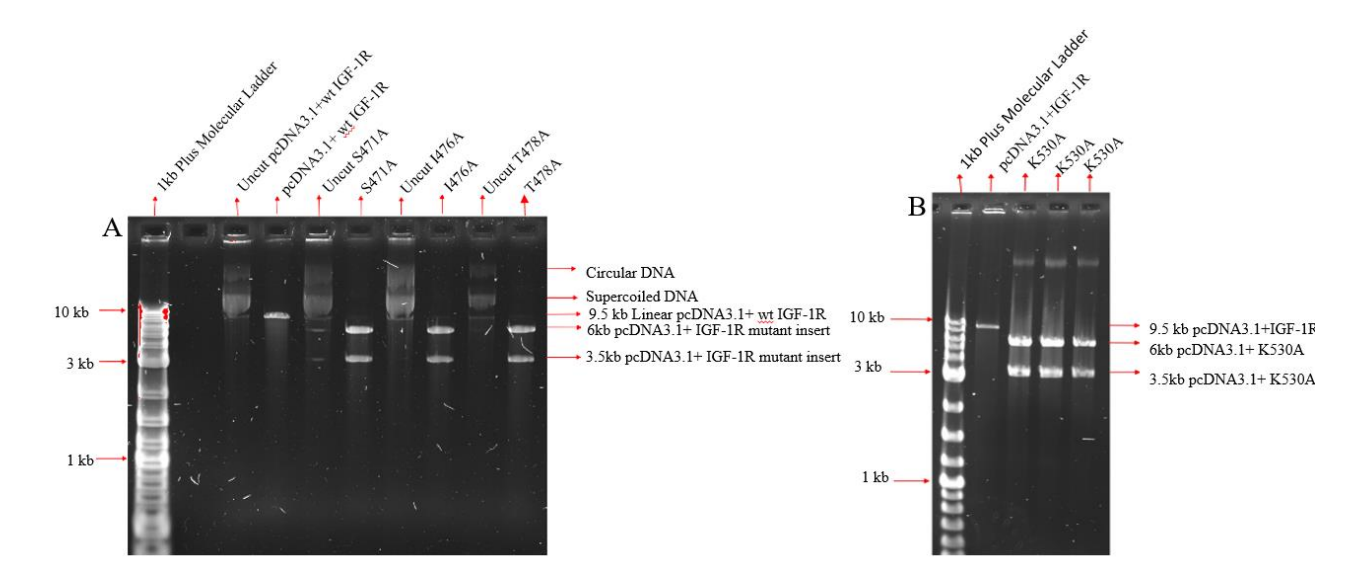


Figure 3.4: Agarose gel electrophoresis showing restriction digestion of pcDNA3.1 vector with IGF-1R mutant constructs. pcDNA3.1 expression vector encoding for IGF-1R mutants was digested with NsiI at 37°C as a method to confirm the presence of mutant. The construct was then run on 0.8% agarose in 1x SB buffer at 100V for 1.5 hours, stained with 3x GelRed dye for 2-5 mins and visualised using ChemiDoc Imaging System. The presence of NsiI silent site in the mutant insert and in pcDNA3.1 vector system helped in confirming the successful ligation of pcDNA3.1 vector with IGF-1R K530A mutant construct by producing two fragments of 6 kb and 3.5 kb. A) Lane 1 represents 1kb Plus Molecular Ladder, Lane 2 represents uncut pcDNA3.1+ wt IGF-1R, Lane 4 represents cut pcDNA3.1+ wt IGF-1R, Lane 5 represents uncut S471A, Lane 6 represents cut S471A, Lane 7 represents uncut I476A, Lane 8 represents cut I476A, Lane 9 represents uncut T478A and Lane 10 represents cut T478A. B) Lane 1 represents 1kb Plus Molecular Ladder (NEB), Lane 2 represents NsiI digested pcDNA3.1 + wt IGF-1R, Lane 3-5 represents NsiI digested pcDNA3.1 + K530A samples.

3.1.5 Sanger sequencing of pcDNA3.1+ IGF-1R FnIII-I domains:

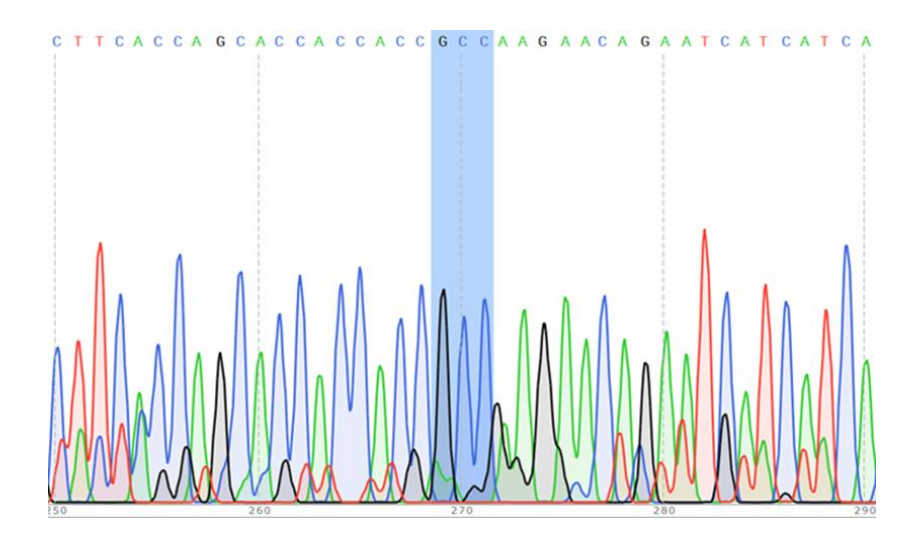


Figure 3.5: Sanger sequencing chromatogram confirming the presence of Ser471Ala (S471A) mutation in the IGF-1R FnIII-I domain construct using ApE software. The cloned mammalian expression vector pcDNA3.1+IGF-1R(S471A) was sent for sanger sequencing and the partial sequence shows successful codon change from S (AGC) to A (GCC).

The vector constructs were purified and sent for sequencing as described in section 2.2.1.7. Sanger sequencing confirmed pcDNA3.1+ IGF-1R(S471A) construct to have the point mutation as evidently demonstrated in figure 3.5. However, the sanger sequence received for pcDNA3.1+ IGF-1R(I476A) was not of good quality. Hence, another sample needs to be sent to confirm the mutant gene fragment integration in pcDNA3.1 expression vector. Similarly, another sample of pcDNA3.1+ IGF-1R(T478A) needs to be sent for sequencing again. The sequence received for T478A mutant gene fragment appeared to be the sequence of wild-type IGF-1R gene fragment instead of mutant fragment. This seemed to be highly unlikely due to the presence of silent site of NsiI restriction enzyme and as there is likelihood of the sequence to be too close to the primer binding site which can lead to some mismatches in this region. Due to time constraints, IGF-1R K530A mutant construct was not sent for sequencing.

3.2 Cellular expression and activation IGF-1R FnIII-I mutant domains

3.2.1 Transfection of pcDNA3.1+ IGF-1R FnIII-I domain mutants into DKO cells:

To access the receptor expression and activation of IGF-1R with point mutations on S471A, I476A and T478A of FnIII-I domain, HEK 293FT double knockout –IR/IGF-1R cell line (DKO cells, a kind gift of A/Prof E. Choi, University of Texas Southwestern Medical Center) was transfected with midi prepared mutant vector construct pcDNA3.1 + IGF-1R S471A, I476A and T478A as described in section 2.2.1.9. One out of two technical replicates of each type of mutant plasmid were stimulated with 10nm of IGF I for 10 mins, and then the cells were lysed after which the lysates prepared were quantified and electrophoresed as described in section 2.2.3.1.

3.2.2 Expression of IGF-1R FnIII-I domain mutant receptors in DKO cells:

The expression of IGF-1R FnIII-I domain mutant receptors in DKO cells determination was the primary objective to analyse the effect the FnIII-I domain mutants had on normal cellular functions. To assess it, the DKO cell lysates were prepared as described in section 2.2.2.5, separated by SDS-PAGE (as described in section 2.2.3.1) and then transferred onto a nitrocellulose membrane as mentioned in section 2.2.3.2. Post the transfer, the proteins were probed with respective primary antibodies as described in section 2.2.3.3. In this case, an anti-IGF-1R beta antibody was used to determine the expression of the mutant receptors on cells.

The outcome of this experiment demonstrated that all FnIII-I domain mutant receptors were expressed in the DKO cells as shown in figure 3.6A as it clearly shows that the signal intensity for IGF-1R receptor protein is similar across the blot. Its corresponding protein gel validates the same as the protein gel acts a loading control and it is evident from figure 3.6A that the amount of protein loaded into the gel was consistent across the gel. Also, when compared to the WT IGF-1R, the mutant receptor samples show greater signals which can be interpreted that there was a greater expression of mutant receptors than the WT IGF-1R receptor. However, there is not much difference in the intensity of signals between the stimulated and unstimulated replicates.

3.2.3 Activation of IGF-1R FnIII-I domain mutant receptors in DKO cells:

In section 3.2.2 and from figure 3.6A, it was confirmed that the IGF-1R FnIII-I domain mutant receptors were getting expressed by the DKO cells. Hence, my next objective was to determine their activation efficiency to understand the binding efficacy of IGF-I to FnIII-I

domain mutants of IGF-1R. For this, the cell lysates were quantified and electrophoresed as described in section 2.2.3.1 and then transferred on to a nitrocellulose membrane as mentioned in section 2.2.3.2. The blot was then probed with anti-phospho- IGF-1R β which is primary antibody binding to pTyr1135/1136 residues of IGF-1R. By performing this blot, I'm trying to determine that can the receptors be activated or not because just a mere expression of the receptor cannot be concluded that the receptor was activated.

From figure 3.6B, it cannot be conclusively said that the receptors can be activated or not due to the presence of weak WT IGF-1R signalling. However, when observing the protein gel image in figure 3.6B, it appears that the amount of protein loaded into gel is similar across the wells.

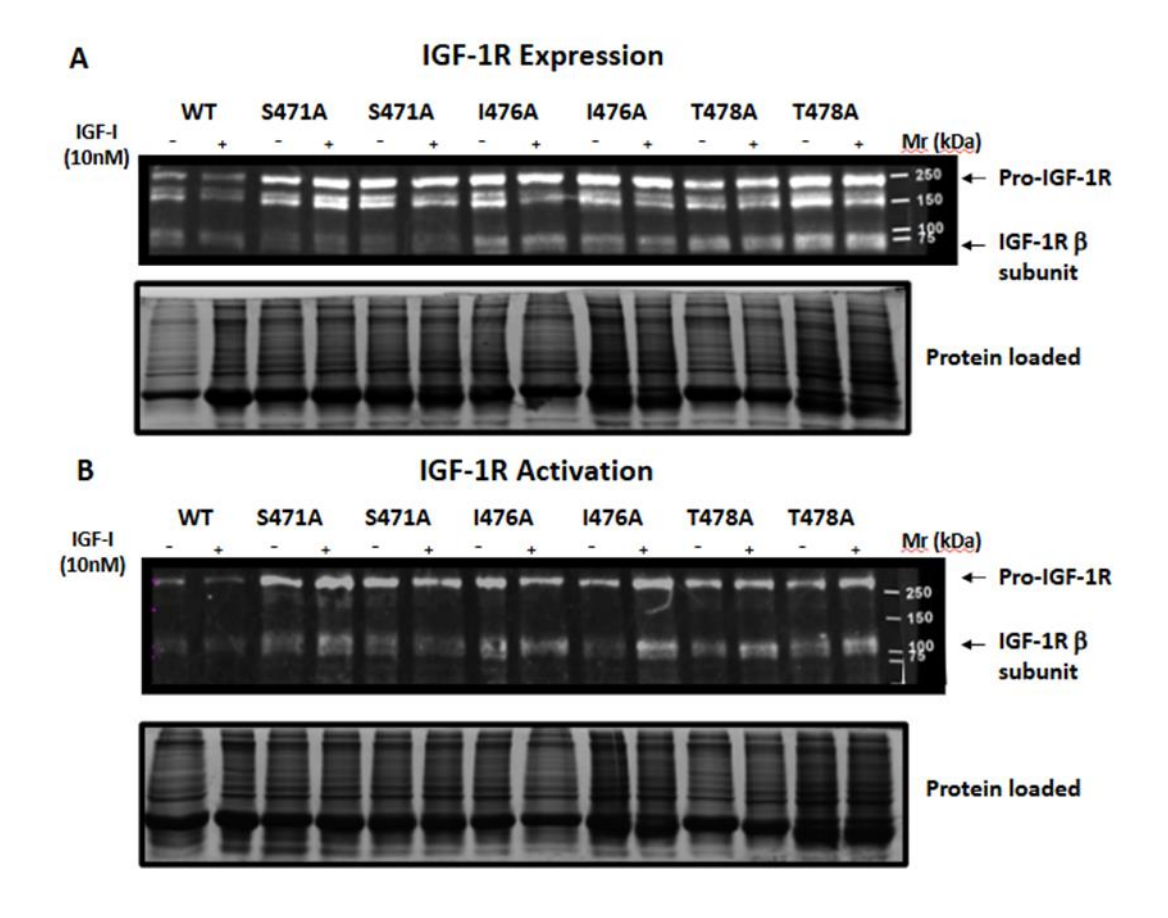


Figure 3.6: Evaluation of IGF-1R expression and activation in wild-type (WT) and mutant receptors. HEK 293FT DKO cells were transfected with IGF-1R WT and mutant receptors and stimulated with 10nM IGF-I for 10 mins. After 10 mins of stimulation, the cells were then lysed, and the lysed samples were prepared according to section 2.2.2.5. Lysates

were electrophoresed on a 10% gel and separated proteins were transferred onto a nitrocellulose membrane according to section 2.2.3.2. A) Western blot analysis showing total expression levels of IGF-1R after probing it with anti-Igf-1R β antibody to detect the precursor (Pro IGF-1R) and mature β -subunit of IGF-1R at 95 kDa. Total protein gel staining served as a loading control. B) Western blot analysis showed IGF-1R activation determined by phosphorylation levels after IGF-I stimulation by probing it with anti-phosphorylated IGF-1R antibody. Total protein gel staining served as loading control.

CHAPTER 4: DISCUSSION

4.1 Successful cloning of IGF-1R FnIII-I domain mutants into mammalian expression vector pcDNA3.1

IGF-1R FnIII-I domain mutants, S471A, I476A, T478A and K530A are anologous to the residues found in IR which have been determined to be significant in binding of insulin at low affinity site of IR. To determine the binding efficacy of these residues present on IGF-1R, they were mutated to alanine, a non-polar amino acid which is widely preferred in site-directed mutagenesis due to small size and non-polarity(Uchikawa et al., 2019).

Four G-blocks of IGF-1R mutants with the proposed mutations were purchased from IDT. They were first cloned into a bacterial cloning vector, pGEM-T easy vector which was then transformed into DH5 α cells. The recombinant plasmid was extracted using miniprep DNA extraction kit from QIAgen which was then double restriction digested with XhoI and KpnI-HF to cut out the mutant gene fragment from the cloning vector. With the same restriction enzymes, the mammalian expression vector, pcDNA3.1+ IGF-1R, was cut to produce the same cut sites. With the help of T4 ligase, the mutant gene fragments were ligated into pcDNA3.1+IGF-1R (-X/K) and transformed into DH5 α cells. The positive colonies were picked and midi prepared. A small sample was used to confirm the ligation of IGF-1R mutant gene fragment into pcDNA3.1+IGF-1R by performing a restriction digestion with NsiI. After the confirmation from restriction digestion, the positive samples were sent for Sanger sequencing.

A lot of troubleshooting and optimization was done to get successful samples of pcDNA3.1+ IGF-1R mutants. By changing several factors affecting such as ligase concentration, insert:vector concentration for ligation, UV light wavelength, new pGEM-T easy kit etc. After several experiments of optimizing the right concentration and combination of the above stated factors, I was able to get successful samples of pcDNA3.1+IGF-1R mutants

4.2 Expression and activation of IGF-1R FnIII-I domain mutants in DKO cells:

HEK 293FT Double knockout –IR/IGF-1R which was a kind gift of A/Prof E. Choi, University of Texas Southwestern Medical Center, was transfected with pcDNA3.1+IGF-1R mutants to determine the expression and activation of the mutant receptors when stimulated with 10nM IGF-I. The cell lysates were quantified for protein concentration and run on gel to separate out

the proteins. The proteins were then transferred onto a nitrocellulose membrane after which, it was blotted with primary and secondary antibodies.

From figure 3.6A, it can be concluded that the mutant receptors were expressed on the cells by examining the signals exhibited by the mutant receptors when compared with the wild type. Despite the fact that, the protein loaded on gel is similar across the wells, the intensity of the signals for expression was varying across the blot. A similar trend is seen in figure 3.6B, wherein the signals for the activation of the receptor was varying across the blot despite the protein loaded on gel looks similar across the wells. Moreover, due to weak signals in the wild type sample for activation of receptor blot, it cannot be concluded regarding the intensity of the activation of the receptor.

This varying result in probing of the blots was mainly caused due to lifting off of cells while serum starvation which can be one of the major reasons for the varying signal intensity.

4.3 Future Direction:

For future directions of this research, the first approach should be to do more technical replicates of this IGF-1R gene mutants. As in this research, only a single technical replicate was able to perform, with the data acquired from more technical replicates using the same IGF-1R gene mutant, one can derive more robust conclusion regarding the change in binding efficacy of IGF-I at low affinity binding site.

Additionally, the receptor proteins should be probed for Akt and ERK downstream signalling pathway to determine the intracellular signalling cascade followed by activation of mutated receptors. This would help in determining which pathway is followed if we mutate the receptor.

For cell culturing, the DKO cells are quite sensitive to serum starvation. Hence, in future, while performing serum starvation gentle handling of the cells should be followed as there is high chance of cells lifting off from the plate. Also, care should be taken regarding the incubation period of serum starvation as in-house laboratory optimised protocol for DKO cells during serum starvation was of 12-16 hours. However, in this research the cells were serum starved for more than 24 hours which can cause a change in their morphology and their viability resulting in varying degree of expression and activation of receptor among the same technical replicates.

Another future direction can be to complete a ligand dose-response with mutant receptors. In this project, I have only used a single concentration of ligand, 10nM IGF-I. Hence, performing

a ligand dose-response experiment, would give an insight to which concentration of ligand can be considered as the minimum concentration where we can get optimum result and draw conclusions for the expression and activation for the mutant receptors for each ligand response.

The final future direction is to perform a combination of mutant receptor expression and activation. In this project, I have performed experiments with single mutated IGF-1R receptors due to which I wasn't able to observe significant difference in the expression and activation of the mutant receptors when compared with wild type receptor. By performing a combination of mutant receptors, there's a higher possibility to get a significant difference in the expression and activation caused due to the mutations made in the receptors.

4.4 Conclusion

This work sought to answer one basic question in growth factor signaling: how does the IGF-1 receptor (IGF-1R) become activated upon binding by its ligands, IGF-I and IGF-II? More precisely, we wanted to know whether or not a region of the receptor known as the FnIII-I domain—is a bona fide "low-affinity" binding site—plays a real, functional part in this activation.

To explore this, we created DNA constructs with care in which we replaced four specific amino acids (Ser471, Ile476, Thr478, and Lys530) with alanine and subsequently introduced these changes in human cells that do not normally synthesize IGF-1R. We used a combination of molecular cloning, protein expression, and signaling assays to contrast the activity of the mutated receptors toward IGF-I stimulation to that of the unchanged, normal receptor.

What we found was surprising. Changes in Ser471, Ile476, and Thr478—residues in the site-2 region as predicted—affected the receptor's ability to get activated, further suggesting that this region indeed plays a part in ligand binding and signal initiation. The mutation of Lys530, lying closer to the main binding site, had an even stronger effect, actually blocking receptor activation. Together, these results support the hypothesis that IGF-1R activation is not a function of one high-affinity site but an organized process through several contact points.

These findings don't merely contribute to our knowledge of how IGF-1R functions—they have implications beyond that. IGF-1R is already known to be involved in most cancers, and knowing how it is activated offers new possibilities for more targeted therapies. Finding out which regions of the receptor are most critical, this study sets the stage for creating drugs that

might be able to more specifically shut down aberrant signaling without interfering with normal growth and metabolism.

Reference

Adams, T., Epa, V., Garrett, T., & Ward*, C. (2000). Structure and function of the type 1 insulin-like growth factor receptor. Cellular and Molecular Life Sciences CMLS, 57, 1050-1093.

Bähr, C., & Groner, B. (2005). The IGF-1 receptor and its contributions to metastatic tumor growth—Novel approaches to the inhibition of IGF-1R function. Growth Factors, 23(1), 1-14.

Belfiore, A., Malaguarnera, R., Vella, V., Lawrence, M. C., Sciacca, L., Frasca, F., Morrione, A., & Vigneri, R. (2017). Insulin receptor isoforms in physiology and disease: an updated view. Endocrine reviews, 38(5), 379-431.

Blyth, A. J., Kirk, N. S., & Forbes, B. E. (2020). Understanding IGF-II action through insights into receptor binding and activation. Cells, 9(10), 2276.

Cai, K., Zhang, X., & Bai, X.-c. (2022). Cryo-electron microscopic analysis of single-pass transmembrane receptors. Chemical reviews, 122(17), 13952-13988.

Favelyukis, S., Till, J. H., Hubbard, S. R., & Miller, W. T. (2001). Structure and autoregulation of the insulin-like growth factor 1 receptor kinase. Nature structural biology, 8(12), 1058-1063.

Ianza, A., Sirico, M., Bernocchi, O., & Generali, D. (2021). Role of the IGF-1 axis in overcoming resistance in breast cancer. Frontiers in cell and developmental biology, 9, 641449.

Khandwala, H. M., McCutcheon, I. E., Flyvbjerg, A., & Friend, K. E. (2000). The effects of insulin-like growth factors on tumorigenesis and neoplastic growth. Endocrine reviews, 21(3), 215-244.

Livingstone, C. (2013). IGF2 and cancer. Endocrine-related cancer, 20(6), R321-R339.

Macháčková, K., Mlčochová, K., Potalitsyn, P., Hanková, K., Socha, O., Buděšínský, M., Muždalo, A., Lepšík, M., Černeková, M., & Radosavljević, J. (2019). Mutations at hypothetical binding site 2 in insulin and insulin-like growth factors 1 and 2 result in receptor-and hormone-specific responses. Journal of Biological Chemistry, 294(46), 17371-17382.

Pavelić, K., Kolak, T., Kapitanović, S., Radošević, S., Spaventi, Š., Krušlin, B., & Pavelić, J. (2003). Gastric cancer: the role of insulin-like growth factor 2 (IGF 2) and its receptors (IGF 1R and M6-P/IGF 2R). The Journal of Pathology: A Journal of the Pathological Society of Great Britain and Ireland, 201(3), 430-438.

Sélénou, C., Brioude, F., Giabicani, E., Sobrier, M.-L., & Netchine, I. (2022). IGF2: development, genetic and epigenetic abnormalities. Cells, 11(12), 1886.

Uchikawa, E., Choi, E., Shang, G., Yu, H., & Bai, X.-c. (2019). Activation mechanism of the insulin receptor revealed by cryo-EM structure of the fully liganded receptor–ligand complex. Elife, 8, e48630.

Whittaker, J., Groth, A. V., Mynarcik, D. C., Pluzek, L., Gadsbøll, V. L., & Whittaker, L. J. (2001). Alanine scanning mutagenesis of a type 1 insulin-like growth factor receptor ligand binding site. Journal of Biological Chemistry, 276(47), 43980-43986.

Xu, Y., Kirk, N. S., Venugopal, H., Margetts, M. B., Croll, T. I., Sandow, J. J., Webb, A. I., Delaine, C. A., Forbes, B. E., & Lawrence, M. C. (2020). How IGF-II binds to the human type 1 insulin-like growth factor receptor. Structure, 28(7), 786-798. e786.

Yan, S., Jiao, X., Li, K., Li, W., & Zou, H. (2015). The impact of IGF-1R expression on the outcomes of patients with breast cancer: a meta-analysis. OncoTargets and therapy, 279-287.

Yunn, N.-O., Kim, J., Ryu, S. H., & Cho, Y. (2023). A stepwise activation model for the insulin receptor. Experimental & Molecular Medicine, 55(10), 2147-2161.

Zhang, Z., Zhang, Y., Lao, S., Qiu, J., Pan, Z., & Feng, X. (2022). The clinicopathological and prognostic significances of IGF-1R and Livin expression in patients with colorectal cancer. BMC cancer, 22(1), 855.